GeoArabia, Vol. 7, No. 1, 2002
Gulf PetroLink, Bahrain

A crustal transect across the Oman Mountains on the eastern margin of Arabia

Ali I. Al-Lazki, Dogan Seber, Eric Sandvol
and Muawia Barazangi, Cornell University

ABSTRACT

The unique tectonic setting of the Oman Mountains and the Semail Ophiolite, together with ongoing hydrocarbon exploration, have focused geological research on the sedimentary and ophiolite stratigraphy of Oman. However, there have been few investigations of the crustal-scale structure of the eastern Arabian continental margin. In order to rectify this omission, we made a 255-km-long, southwesterly oriented crustal transect of the Oman Mountains from the Coastal Zone to the interior Foreland via the 3,000-m-high Jebel Akhdar. The model for the upper 8 km of the crust was constrained using 152 km of 2-D seismic reflection profiles, 15 exploratory wells, and 1:100,000- to 1:250,000-scale geological maps. Receiver-function analysis of teleseismic earthquake waveform data from three temporary digital seismic stations gave the first reliable estimates of depth-to-Moho. Bouguer gravity modeling provided further evidence of depths to the Moho and metamorphic basement.

Four principal results were obtained from the transect. (1) An interpreted mountain root beneath Jebel Akhdar has a lateral extent of about 60 km along the transect. The depth-to-Moho of 41 to 44 km about 25 km southwest of Jebel Akhdar increased to 48 to 51 km on its northeastern side but decreased to 39 to 42 km beneath the coastal plain farther to the northeast. (2) The average depth to the metamorphic basement was inferred from Bouguer gravity modeling to be 9 km in the core of Jebel Akhdar and immediately to the southwest. A relatively shallow depth-to-basement of 7 to 8 km coincided with the Jebel Qusaybah anticline south of the Hamrat Ad Duru Range. (3) Based on surface, subsurface, and gravity modeling, the Nakhl Ophiolite block extends seaward for approximately 80 km from its most southerly outcrop. It has an average thickness of about 5 km, whereas ophiolite south of Jebel Akhdar is only 1 km thick. The underlying Hawasina Sediments are between 2 and 3 km thick in the Hamrat Ad Duru Zone, and 2 km thick in the Coastal Zone. (4) Southwest of Jebel Akhdar, reactivated NW-oriented strike-slip basement faults that deformed Miocene to Pliocene sediments were inferred from the interpretation of seismic reflection profiles.

INTRODUCTION

Location and Tectonic Setting

The study area in northern Oman (Figure 1) includes part of the eastern margin and foreland of the Arabian Plate. Tectonically, the most prominent feature is the Oman Mountains, also known as the Hajar Mountains, that have a length of about 700 km, a width varying between 40 and 130 km, and elevations of up to 3,000 m above sea level.

Plate boundaries of several different types delineate the Arabian Plate (Figure 1). In the west, a divergent boundary extending through the Red Sea and into the Gulf of Aden marks stages of early continental rifting (northern Red Sea) to the final stages of development of a mature oceanic lithosphere (southern Red Sea and Gulf of Aden). In the northwest, the sinistral Dead Sea transform fault system separates the Arabian Plate from the Sinai and Levantine subplates of the African Plate. The northern and the northeastern boundaries are continent-continent collision zones between the Arabian and the Eurasian plates along the Bitlis and the Zagros sutures. The Zagros suture continues south and transforms into the continent-oceanic Makran subduction zone. The Owen and Murray transform faults mark the southeastern boundary of the Arabian Plate with the Indian Plate.

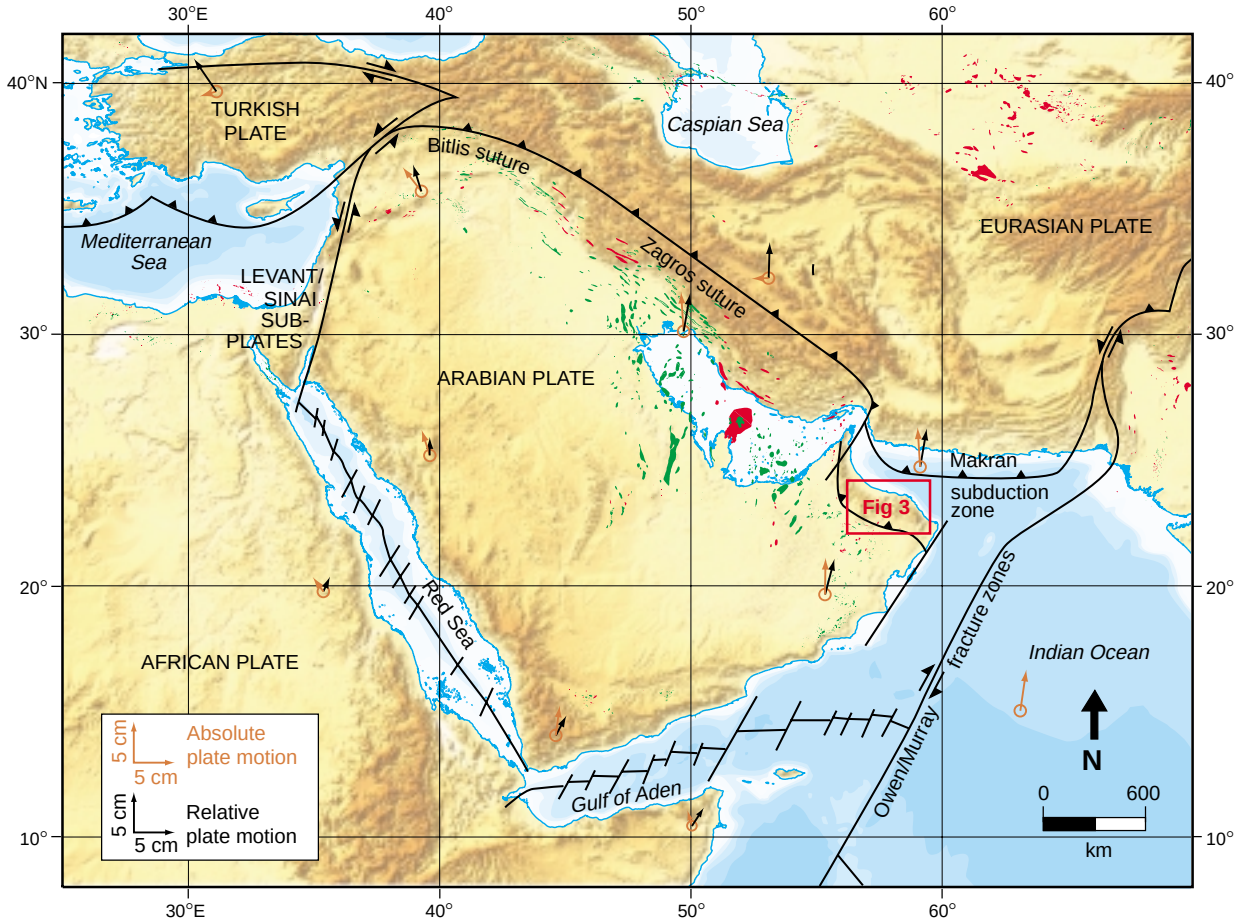

Figure 1: Simplified plate tectonic setting of the Arabian Plate. Oil (green) and gas (red) fields are shown. Base map from Sharland et al. (2001); plate motion after Kensaku Tamaki, Ocean Research Institute, University of Tokyo [http://manbow.ori.u-tokyo.ac.jp].

Previous Geophysical Studies

Only a few geophysical studies have been made of the eastern Arabian margin and continental crust in Oman. That by Manghnani and Coleman (1981) was based on 2-D Bouguer gravity modeling and gave an estimate for the average crustal thickness of about 40 km, with a maximum thickness of about 43 km below Saih Hatat. Recent work by Ravaut (1997) and Ravaut et al. (1997) provided an estimate for the average crustal thickness of about 43 km on the eastern margin of Arabia and a maximum thickness of about 47 km beneath the Oman Mountains. Their studies were based primarily on the modeling of Bouguer gravity data together with limited subsurface information and constraints.

GEOLOGIC SETTING

Five tectonic sequences are recognized in Oman (Figure 2). They are: (1) pre-Permian, (2) the Hajar Supergroup, (3) the Allochthonous Sequence (Semail Ophiolite and Hawasina Sediments), (4) the Aruma Group, and (5) Tertiary Cover Sequence.

Rifting events that began in the Precambrian / Cambrian and Early Permian led to the development of the distinctive sequences of the pre-Permian (late Proterozoic to Early Permian) alternating clastics and carbonates, and the Hajar Supergroup (Late Permian-mid Cretaceous) composed predominantly of marine carbonates.

The emplacement of Late Cretaceous ophiolites was one of the most important tectonic events to have affected the eastern margin of the Arabian Plate (Glennie et al., 1973; Boudier and Coleman, 1981;

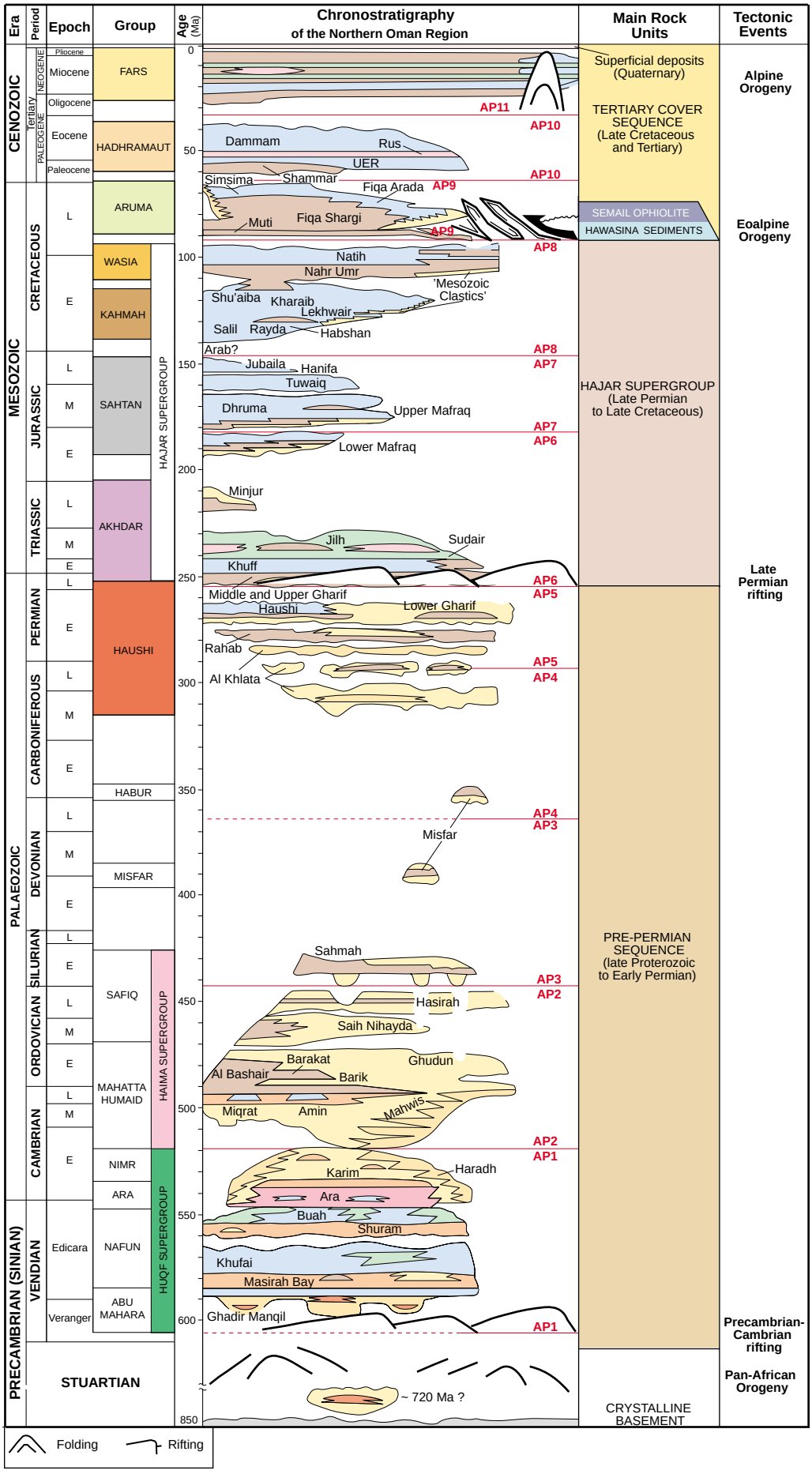

Figure 2: Geologic column of northern Oman showing major sedimentary groups (ARUMA) and key formations (Muti), and major tectonic events that have affected the eastern Arabian margin and surrounding region. Modified from Naylor and Spring (2001) and Le Métour, Mitchel et. al. (1995). Arabian Plate (AP) tectonostratigraphic megasequence boundaries from Sharland et al. (2001).

Coleman, 1981; Lippard, 1983). This tectonic event led to the emplacement of the Allochthonous Sequence consisting of the 10- to 12-km-thick Semail Ophiolite (Shelton, 1990) and deep oceanic and shallow-marine sediments of the Mesozoic Hamrat Ad Duru and Sumeini groups, respectively. The emplacement event spanned the Cenomanian to Coniacian stages (Hopson et al., 1981; Pallister and Hopson, 1981; Boudier et al., 1985; Nicolas et al., 1996; and Searle and Cox, 1999). Bechennec et al. (1995) recorded the ophiolite advance in the foreland region. In this paper, we refer to both the Hamrat Ad Duru and Sumeini groups as the Hawasina Sediments. Units of the Muti Formation deposited during the Turonian-Coniacian / Santonian mark the transition from a passive continental margin to a foreland basin (Robertson, 1987; Bechennec et al., 1995).

The syntectonic Aruma Group (Fiqa Formation) was deposited during the Campanian to Maastrichtian. In this study, we considered the Fiqa and Muti formations separately when establishing stratigraphic relationships, but jointly as the Aruma Group when establishing regional lateral continuity (Figures 2 and 4). Finally, the post-emplacement period was followed by the deposition of the Tertiary (Tertiary and Quaternary) cover rocks, and the Miocene Zagros collision event.

Two prominent domal structures in the Oman Mountains are the 3,000-m-high Jebel Akhdar, and Saih Hatat (Figure 3). They provide a window onto the stratigraphy of the pre-Permian and Hajar Supergroup sequences and have been intensively investigated with regard to the timing and mechanism of deformation. Several alternative models have been proposed. One model is of a fault-bend fold style of deformation (e.g., Cawood et al., 1990; Hanna, 1990) but the proposed geometry and the existence of the fault-bend fold are controversial. Le Métour, Bechennec and Roger (1995) concluded that the structures of Jebel Akhdar and Saih Hatat were probably inherited from Late Permian horst-and-grabens at the edge of the continental shelf. Mount et al. (1998) suggested that Jebel Akhdar was the result of a compressional event that began in the Oligocene and involved a high-angle reverse fault (a fault-propagation fold) below the southern limb of the mountain. We found that the present-day structure of Jebel Akhdar could not be described by a single deformation style or by a single event, but was the result of the interplay of various multiple events.

CRUSTAL TRANSECT

The main objective of our study was to construct a crustal-scale transect across the eastern Arabian margin, from the Coastal Zone, through the Oman Mountains, and into the interior Foreland. Geographically, the transect starts offshore, crosses the coastal plain and the Jebel Akhdar mountain range in a southwesterly direction, and ends in the interior of Oman, southeast of the Natih and Fahud structures (Figure 3). The multidisciplinary approach we used integrated data and results from the following sources: (1) seismic reflection and well-data interpretation; (2) earthquake receiver function analysis; and (3) Bouguer gravity models. We used 2-D seismic reflection profiles and well data to constrain the upper 8 km of the crust, the receiver function to infer depth-to-Moho at three locations, and Bouguer gravity modeling to further constrain the lateral extent of the Moho and to infer the depth to the metamorphic basement.

We divided the transect into four structural zones from north to south as follows:

(1) The Coastal Zone (and offshore area) north of Jebel Akhdar.
(2) The Mountain Zone, corresponding to the Jebel Akhdar range.
(3) The Hamrat Ad Duru Zone south of Jebel Akhdar, which has the most intensive surface deformation within the Hawasina Sediments.
(4) The Interior Zone, which shows minimal surface deformation south of Jebel Qusaybah (see Figure 3).

We grouped the Interior Zone and Hamrat Ad Duru Zone as the Foreland, and the Mountain Zone and Coastal Zone as the Hinterland.

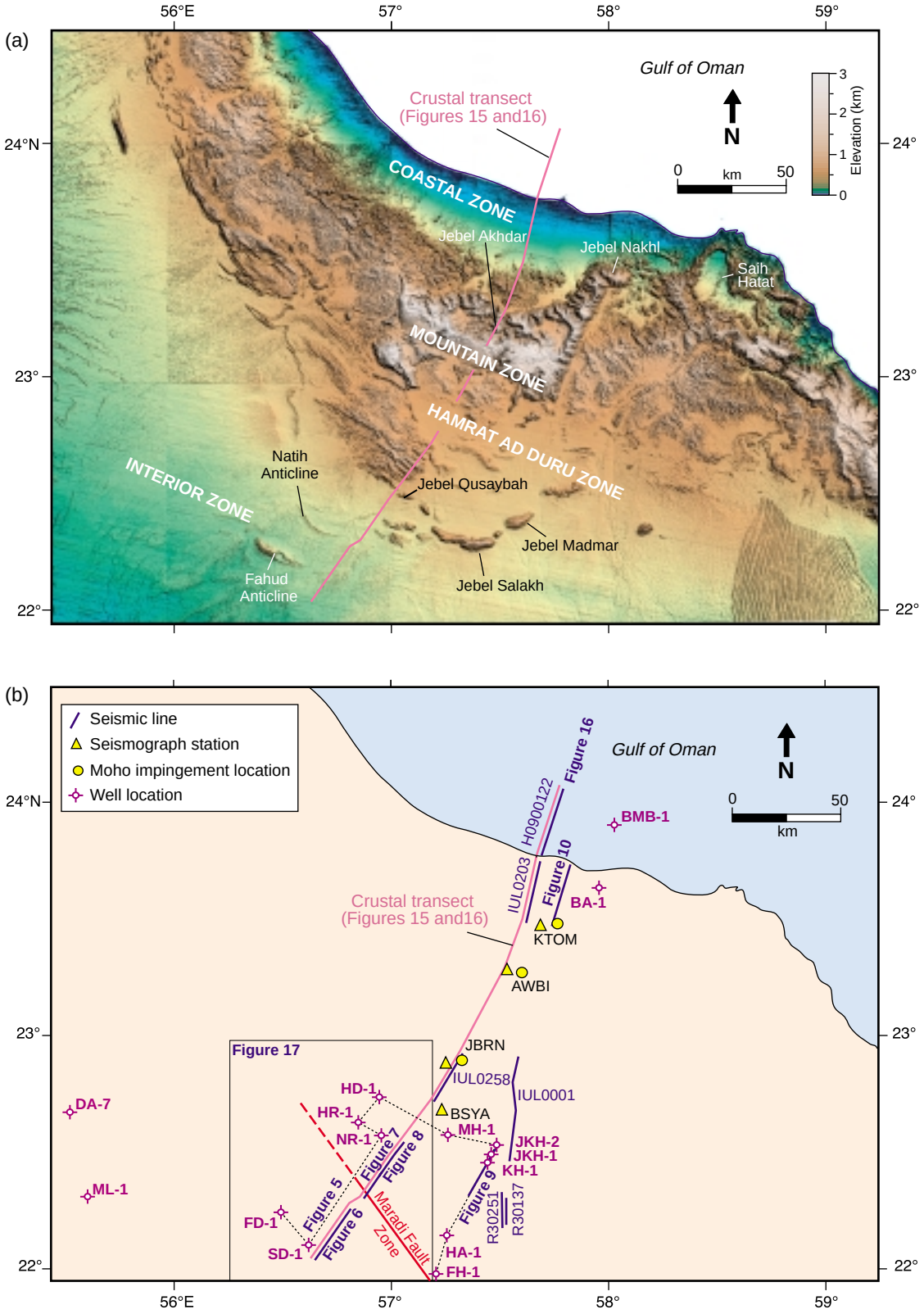

Figure 3: Topographic map of the study area showing (a) location of crustal transect, and (b) seismic reflection lines, seismograph stations, and wells (see Figure 1 for location). The base map in (a) is a shaded relief representation of topography available from Cornell University.

Seismic Reflection and Well Analysis

Data

Data used in the seismic interpretation consisted of 152 km of 2-D reflection profiles along the transect (Figure 3), 100 km of which were in digital form and 52 km were analog paper copies. Seismic reflection data processing involved depth conversion of the 2-D seismic profiles using stack and migration velocities. These methods were also used to perform line-depth conversion on the analog data. Data from 15 exploratory wells were used to identify and correlate with stratigraphic units mapped from the seismic reflection profiles (Figure 3). Well data consisted of information on formation tops, age, lithology, and biostratigraphy prepared by various oil companies for exploration purposes. We also had available the 1:100,000-scale and 1:250,000-scale geologic maps of Oman (Bechennec et al., 1986a, b; Beurrier et al., 1986; Chevrel et al., 1992; Rabu et al., 1986; Wyns et al., 1992) from which to construct a geologic cross-section. The maps provided lithological, age, and—most importantly—dip information for the Jebel Akhdar range where no seismic or exploratory well information was available.

Methods

Seismic reflection profiles directly on the transect gave the most complete coverage in the Interior Zone and the Coastal Zone. Seismic correlation and interpretation provided important information on the stratigraphic and structural relations of the Hajar Supergoup and the overlying sequences. We have limited confidence in the correlation of the pre-Permian Sequence at depths below 3 sec two-way

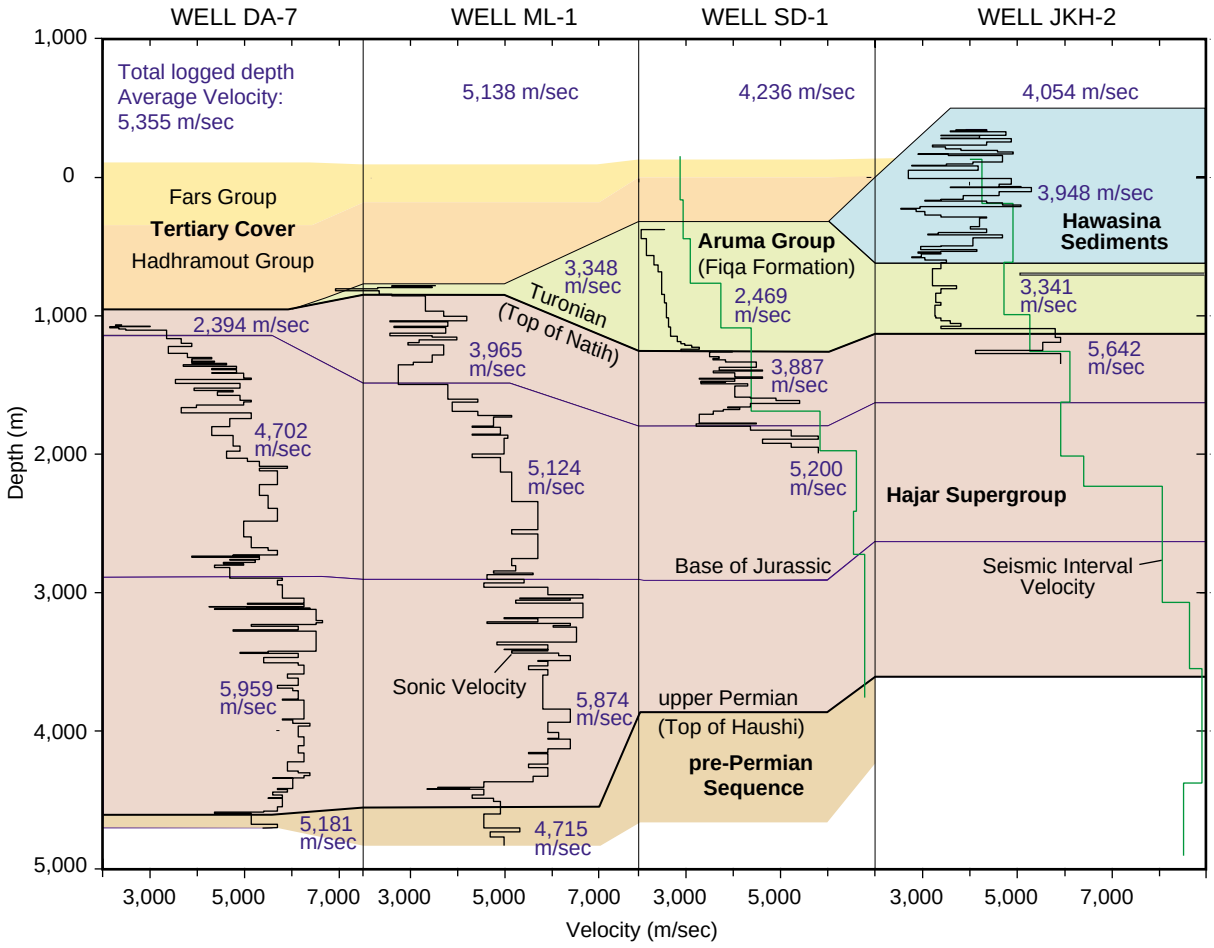

Figure 4: Well-log correlation diagram: sonic velocities as black lines and interval seismic velocities in green. Seismic interval velocities overlain on SD-1 and JKH-2 were obtained from lines S50295, and IUL0001, respectively (see Figure 3). Blue numbers are the averaged velocities for designated intervals.

travel time (TWT) that corresponded approximately to the top of the Lower Cambrian Huqf Group. The top of metamorphic basement was almost impossible to identify in the Interior, Hamrat Ad Duru, and Coastal zones. Depth-converted time sections using interval stack and migration velocities showed in some cases a depth difference of about 200 to 300 m at the 1 sec TWT level, and deeper levels (Figure 4).

Information from wells was used to correct the depth-converted seismic sections wherever wells coincided with seismic lines. Where this was not possible, we made sure that the depth-converted seismic section correlated with nearby wells and with wells across the transect. Of the well on or near to the crustal transect, only JKH-2 and SD-1 provided sonic velocity data, but to a maximum depth about 1 km (Figure 4). This deficiency prevented us from further comparing depth-conversion velocities with sonic-velocity data from well logs. Wells DA-7 and ML-1, located respectively 150 km and 100 km west of the transect, provided sonic velocity information for the whole Hajar Supergroup and were important in approximating depth conversion differences with migration and stack velocities (Figure 4). The sonic velocity of the upper part of the Hajar Supergroup (Figure 4), marked by top Natih and base Jurassic, was 4,700 m / sec (well DA-7) and 5,120 m / sec (well ML-1), respectively. The discrepancy was attributed to the lateral thickness variation of some lithologic units. The lower part of the Supergroup, marked by base Jurassic and top Haushi, showed only a small sonic velocity difference in the two wells for an average velocity of about 5,900 m / sec

Well Correlation (Foreland Region)

Well data provided good lateral correlation for the Hajar Supergroup, the Aruma Group, the Hawasina Sediments, and the Tertiary cover rocks in the Foreland region (Figure 5). In addition, the tops of the Haushi, Haima, and Huqf groups that constitute the pre-Permian Sequence were penetrated in wells FD-1 and FH-1.

The top of the Albian Natih Formation marks the top of the Hajar. The full thickness of the Supergroup was about 2.4 km (Figure 5) in the Hamrat Ad Duru Zone (well MH-1), and in the Interior Zone it varied from about 2.6 km in wells FD-1 and SD-1 to about 2 km in well FH-1.

In the Foreland region, the Aruma Group was identified in well data as the Fiqa Formation only, with no mention of the Muti Formation. The age of the Fiqa Formation from well data is Turonian-Maastrichtian, which encompasses with the age of the Muti Formation as mapped at the surface by Chevrel et al. (1992). In some wells the Fiqa Formation is identified as the 'Shargi shale member', and in others simply as a claystone (HD-1 and MH-1). The Formation thickness varies throughout the Foreland (Figure 5). Its average thickness is 595 m along the correlation section of wells HD-1, MH-1, and JKH-2, but in wells JKH-1 and KH-1 it is more than twice as thick (maximum 1,350 m). Such variations in thickness over short distances could be attributed to either localized structural thickening of the unit in wells JKH-1 and KH-1, possibly by reverse faulting, or to misidentification of the Fiqa Formation with the Hawasina Sediments.

The Hawasina Sediments directly overlie the Aruma Group and occur primarily in the Hamrat Ad Duru Zone. They extend as far as well NR-1 at the boundary of the Hamrat Ad Duru with the Interior Zone where they are 154 m thick (Figure 5). The Sediments consist of imbricated stacks of alternating sheets of overthrust Guwayza sandstone and limestone, and thrust sheets of the underlying Aruma Group (Robertson, 1987). For the purpose of sequence correlation we have included the cumulative thickness of thrusted sheets of the Aruma Group with its in place thickness (Figure 5). Well data from the Hamrat Ad Duru Zone do not include the Tertiary Cover Sequence; only wells SD-1 and FH-1 in the Interior Zone contain Tertiary sediments.

Well Correlation (Coastal Zone)

Few exploration wells have been drilled in the Coastal Zone and offshore area. Wells BA-1 and BMB-1 (see Figure 3 for location) provided the only well data for the coastal and offshore areas. Well BA-1 located about 30 km east of the transect penetrated the basal parts of the Paleogene Hadhramout Group (Thanetian-Bartonian) at a maximum depth of 2,448 m. Well BMB-1 located 30 km northeast of BA-1 had a maximum depth of 4,631 m. Its location and lateral structural complexity prohibited its

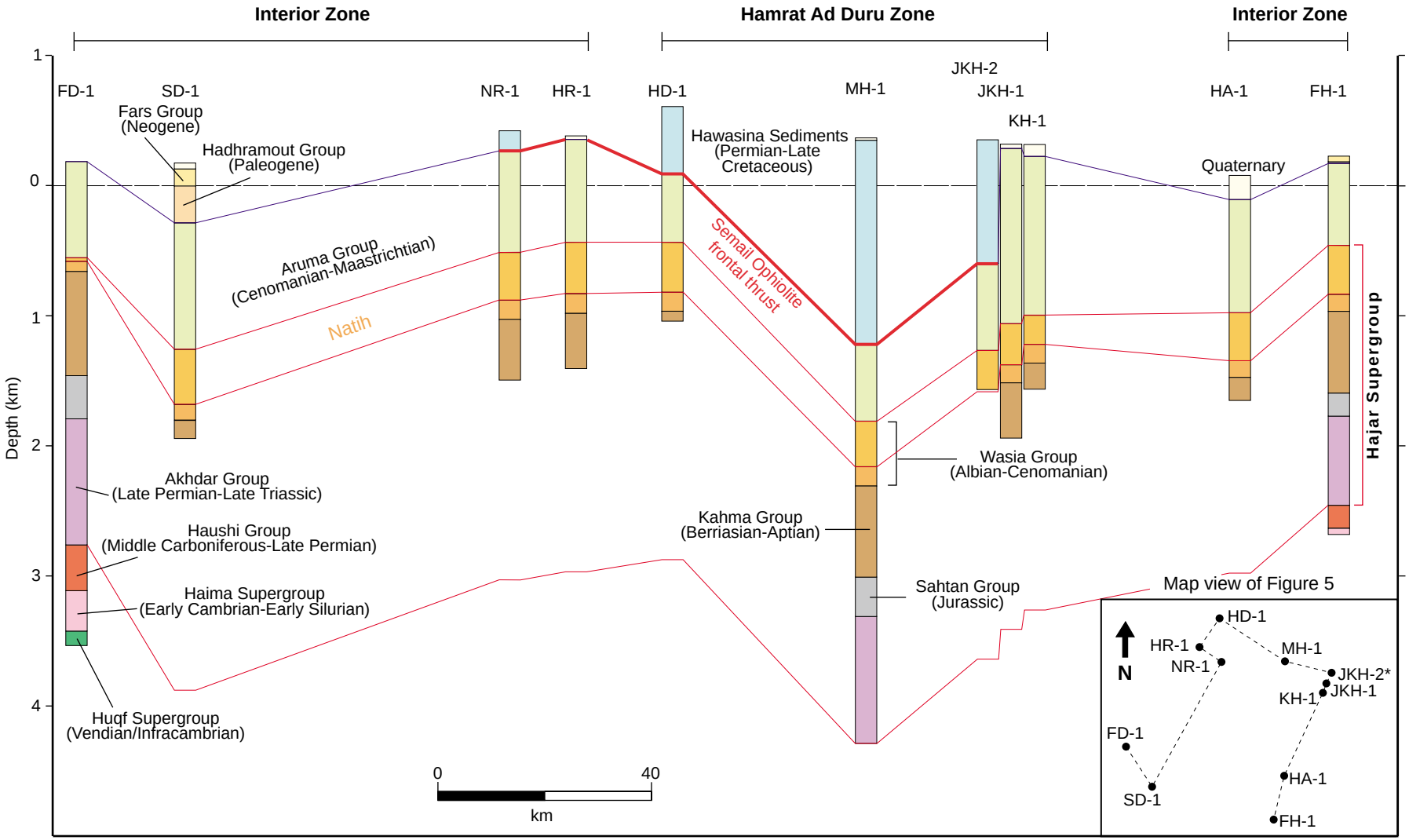

Figure 5: Fence diagram showing correlation of the Hajar Supergroup in the Interior and Hamrat Ad Duru zones (see Figure 3 for location). Red lines represent correlation between units within the Hajar Supergroup, and the blue line marks the top of the Aruma Group (Muti and Fiqa formations). The Semail Ophilite frontal thrust is shown at the sole of the Hawasina Sediments. Age and stratigraphic identification is based on interpretations by oil exploration companies. Stratigraphy after Rabu et al. (1986); Nolan et al. (1990); Pratt and Smewing (1990); Le Métour, Michel, et al. (1995).

projection onto the transect. It is noteworthy that well BMB-1 penetrated 1,195 m of shale, marly sand, and shaley marl of Maastrichtian-Campanian age equivalent to the Alkhawd Formation. It was overlain by only 305 m of the Hadhramout Group, which in BA-1 was 1,200 m thick.

Seismic Interpretation

Interior Zone: Line S50295 (Figure 6)

The upper 1 sec (TWT) of line S50295 consists of the Tertiary Cover Sequence and the Aruma Group (Fiqa and Muti formations) that overlie the Hajar Supergroup. In this and other 2-D reflection profiles, the top of the Muti Formation is inferred from downlapping reflectors of the overlying Fiqa Formation. The reflectors provide a structural relationship between the interpreted Muti and the Fiqa, and are not a distinctive representation of the chronostratigraphy of the Muti Formation. In line S50295, the Fiqa shows a southwesterly reflector progradation, onlapping the top of the Muti. The green reflector at about 200 msec marks the termination of prograding reflectors to be overlain by conformable strata of the Tertiary Cover. Generally, the Aruma Group thickens toward the northeast, but the basal Muti Formation is interpreted as thickening southwestward.

A system of negative flower structures was observed in line S50295 and other 2-D seismic profiles throughout the Interior Zone, and also in parts of the Hamrat Ad Duru Zone. The flower structures in line S50295 show minimal vertical displacement with subtle reflector offsets at the top of the Natih Formation, and gentle folding in the overlying Aruma Group and Tertiary Cover. Below about 2 sec (TWT), the structures converge into a single steep fault that offsets the tops of the Haushi Group (Upper Permian) and Huqf Group (Lower Cambrian) marker reflectors. Fault continuity or surface exposure, especially for the two flower structures in the northeastern part of the profile is obscured within the Fiqa Formation. Alternatively, the fault tips may be within the shales of the Fiqa Formation and did not cross into the Tertiary. However, the base of the Tertiary Cover reflector (green) of the Hadhramout Group does show gentle folding near the surface.

Interior Zone: Line S50274 (Figure 7)

In line S50274 the distinctive reflector markers at the top of the Natih Formation and the top of the Haushi Group clearly delineated the Hajar Supergroup. The Muti Formation top was interpreted at about the 0.9 sec (TWT) level at the northeastern end of line S50274 and at about 1.35 sec in the southwest.

Hanna and Nolan (1989) interpreted the Maradi Fault Zone as a right-lateral strike-slip fault reactivated in Pliocene-Pliestocene times. In line S50274 we interpreted it as being a basement-associated, right-lateral strike-slip fault that included a reverse component. The reverse component was inferred from the 0.35 to 0.4 sec (about 900 m) time difference in the Natih reflector marker across the fault zone . Internal collapse at distances from 2 to 6 km, possibly by normal faulting, occurs toward the center of the structure. In line S50274, the northeastern arm of the central part of the fault zone separates outcrops of the Fiqa Formation to the northeast from the steeply dipping (72ºS) Eocene Umm Er Radhuma Formation and the Miocene-Pliocene Berzman Formation of the Tertiary Cover Sequence.

The relative thickness of the Aruma Group and the Tertiary Cover Sequence on the southwestern side of the Maradi Fault Zone is about 1.6 sec (TWT), whereas to the northeast Fiqa Formation has a relative thickness of about 1.2 sec (TWT). In the southwest, the thickness of the Aruma Group and the Tertiary Cover is correlated with the thickening (1.3 sec) observed at the northeastern end of interpreted line S50295 (Figure 6). Therefore, we interpreted the Maradi Fault Zone to include a reverse faulting component, possibly related to the Late Cretaceous ophiolite emplacement process. The deformation was followed by a transtensional strike-slip faulting event in the Pliocene-Pliestocene, as dated by Hanna and Nolan (1989).

Interior Zone: Line R40984 (Figure 8)

Directly north of line S50274 (Figure 7) is line R40984; the two have about 8 km overlap. Correlation between the two lines is possible as reflectors are subhorizontal and no significant deformation exists in the overlap area. In line R40984, the top of the Hajar Supergroup is distinct in the southwestern section as far as its intersection with the subsurface structure of Jebel Qusaybah. The top of the Hajar

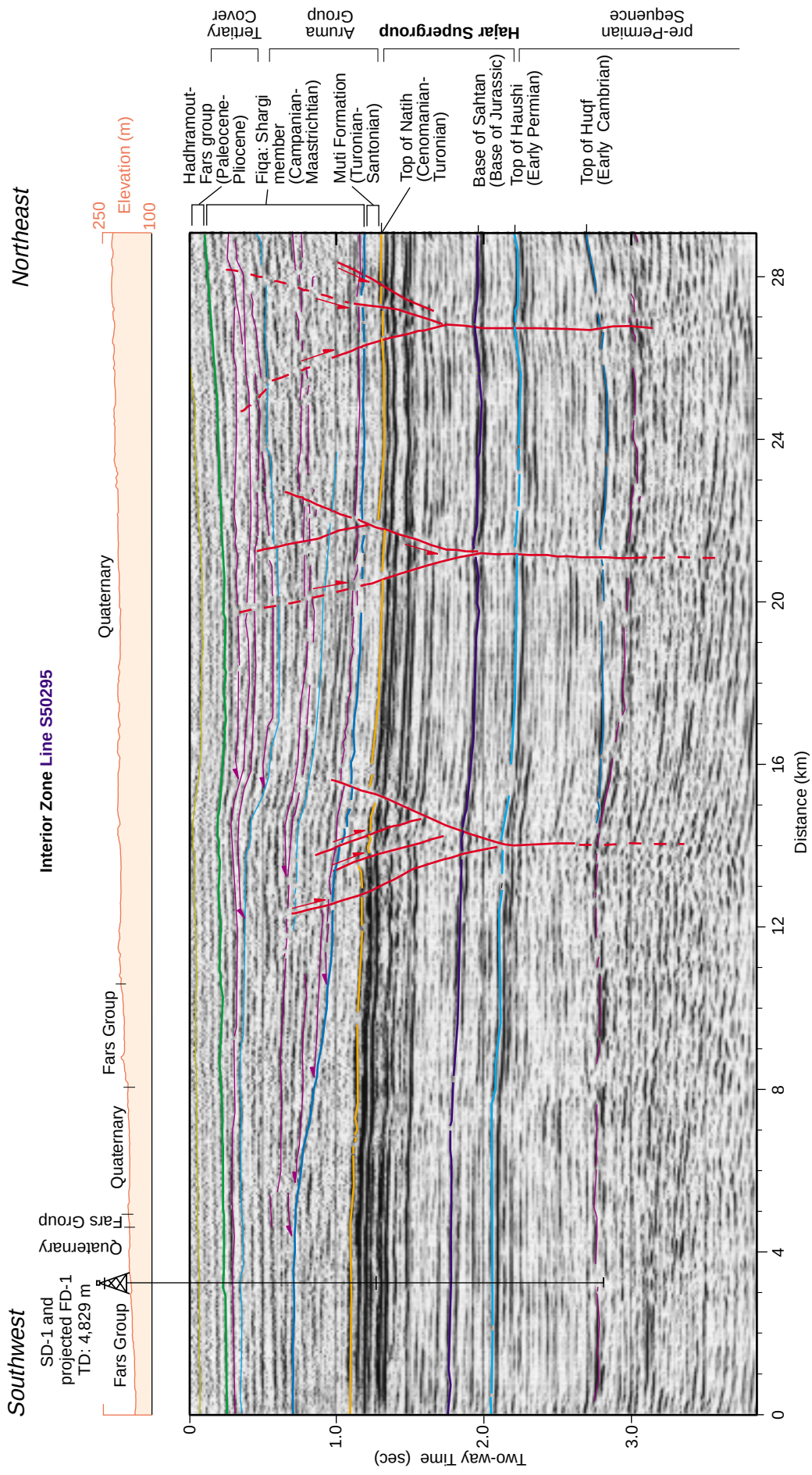

Figure 6: Interpretation of a migrated 2-D seismic reflection profile line S50295 (see Figure 3 for location). Red lines are inferred normal faults with possible continuation shown as dashed lines. The normal fault system forms negative flower structures that offset reflectors below 3 sec. These flower structures are associated with a wrench-fault system in the Foreland region. The upper 1 sec of the section shows reflectors of the Fiqa Formation onlapping southwestward. The orange line represents the top of the Hajar Supergroup.

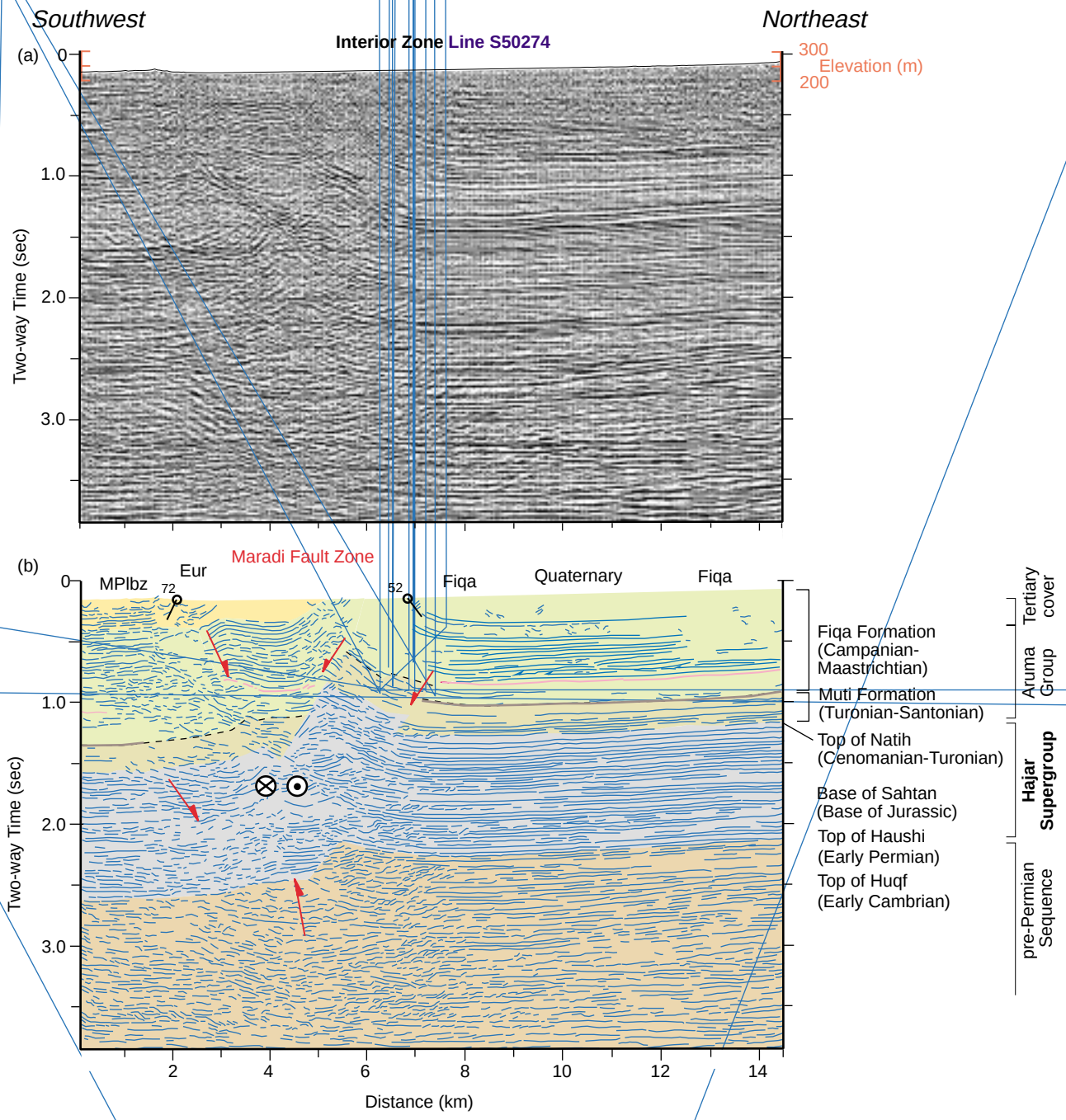

Figure 7: (a) Migrated 2-D seismic reflection profile of line S50274 crossing the Maradi Fault Zone (see Figure 3 for location). (b) An interpretation of seismic line S50274 showing marker reflectors and relative motion within the Maradi Fault Zone. The fault zone has two styles of deformation: a strike-slip component (flower structure) and a reverse component inferred from the depth difference of the Natih Formation reflector (orange line) across the fault zone. Dip information is shown at surface in (b). MPlbz = Miocene-Pliocene Berzman Formation; Eur = Eocene Umm Er Radhuma Formation. Wrench faults: away from observer ⊗; toward observer ⊙.

Supergroup then becomes less obvious and its interpretation is based on correlation with the northeastern side of Jebel Qusaybah and surface outcrops. Only the Aruma Group overlies the Hajar sequence in this section. The Jebel Qusaybah anticline is part of an arc-shaped range of hills that extends westward from Jebel Madmar (Figure 3). In this section, Jebel Qusaybah separates the southernmost extent of the Hawasina Sediments in the Hamrat Ad Duru Zone from the Interior Zone.

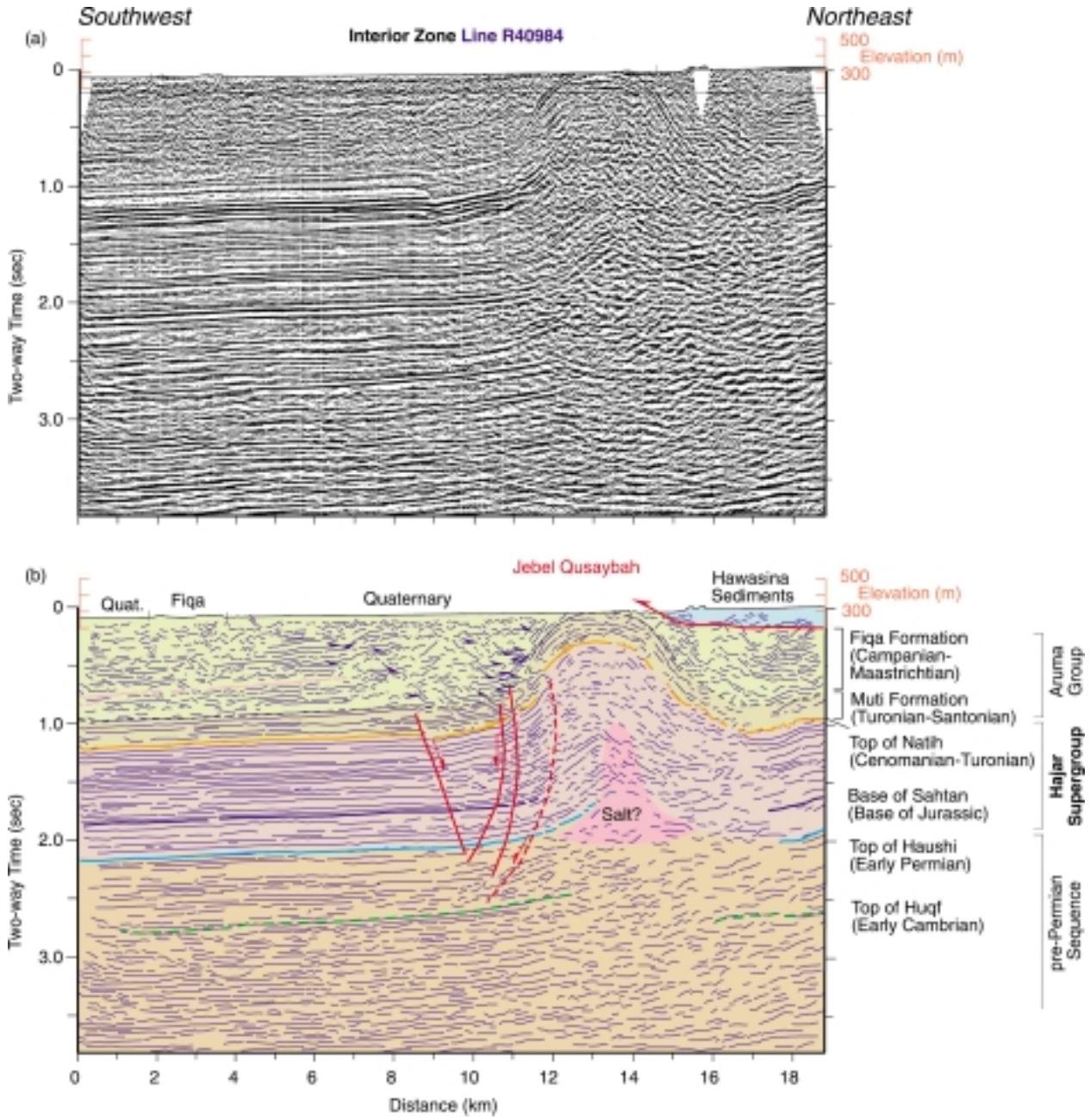

Figure 8: (a) Migrated 2-D seismic reflection profile of line R40984 across the Jebel Qusaybah anticline (see Figure 3). (b) A interpretation of seismic line R40984 showing a normal fault system southwest of Jebel Qusaybah. A zone of strike-slip faulting (flower structure) is interpreted south of Jebel Qusaybah. A bold red line delineates the Semail Ophiolite frontal thrust at the sole of the Hawasina Sediments.

The Jebel Qusaybah anticline shows subsurface symmetry indicated by the top of Hajar Supergroup marker reflector at about 1 sec (TWT) on both sides of Jebel Qusabah. We interpreted the anticline as being supported by a possible salt intrusion into the host rock at about 2 sec (TWT) (Figure 8b). A set of normal faults is interpreted to affect the western limb of the Jebel Qusaybah anticline and the faults may be related to the event that formed the negative flower structures observed in line S50295 (Figure 6). The Fiqa Formation reflectors onlap the southwestern limb of the Jebel Qusaybah structure. Reflectors at the base of the Fiqa are also interpreted to downlap the top of the Muti Formation and prograde toward the southwest.

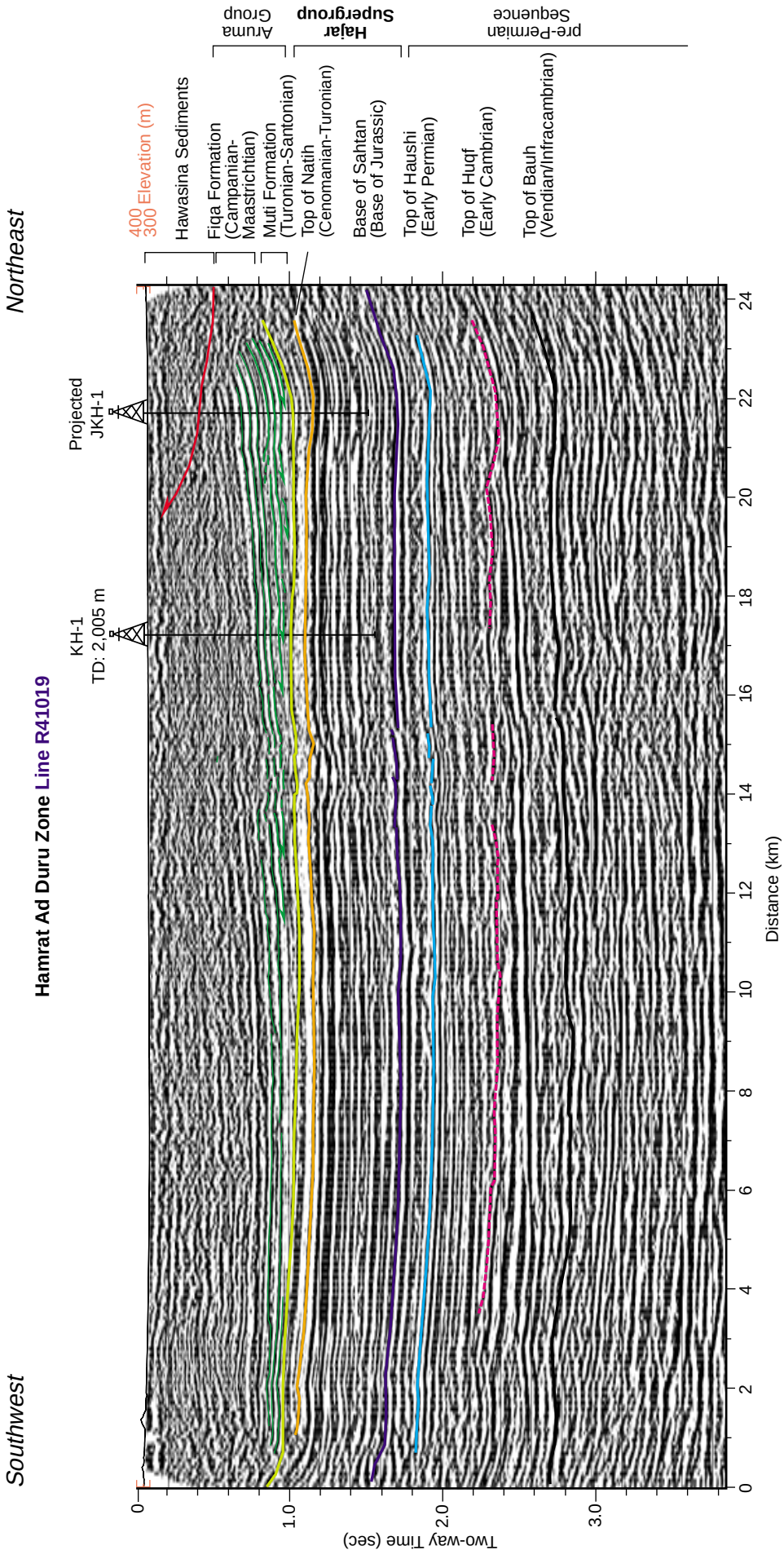

Figure 9: Migrated 2-D seismic reflection profile of line R41019 in the Hamrat Ad Duru Zone with interpretation (see Figure 3 for location). Reflectors of the Fiqa Formation downlap onto the top of the Muti Formation in a southwesterly direction. Important stratigraphic markers are shown.

Hamrat Ad Duru Zone: Line R41019 (Figure 9)

Line R41019 is located east of the transect in the Hamrat Ad Duru Zone. It has the highest signal-to-noise ratio and shows the best stratigraphic relationships within the Aruma Group. In this profile, the Natih Formation reflector at about 1.2 sec (TWT) marks the top of the Hajar Supergroup and its base is the top Haushi Group (Late Permian) reflector at about 2 sec. The Supergroup shows only minor changes in thickness compared to the those of the Interior Zone. The top of the Hajar was identified in seismic profiles throughout the Hamrat Ad Duru Zone, which establish its continuity with outcrops on the southern limb of Jebel Akhdar. Line R41019 also shows the tops of the Huqf Group (Lower Cambrian) and the Buah Formation (Vendian / Infracambrian).

Downlapping reflectors of the Fiqa Formation mark the top of the Muti Formation, which was thinner than previously interpreted from profiles in the Interior Zone. The downlapping reflectors of the Fiqa Formation (dark green) show steeper dips, especially in the northern half of the line. The downlapping reflectors indicate progradation toward the southwest.

Coastal Zone: Line IUL0205 (Figure 10)

A gap in the coverage of seismic and well data across the Jebel Akhdar range limited the subsurface interpretation. To provide constraints, we used structural information from 1:200,000-scale geological maps to correlate the pre-Permian Sequence, the Hajar Supergroup, and overlying units, across the Mountain Zone.

In the Coastal Zone we interpreted line IUL0205 rather than the transect line IUL0203. Line IUL0205 is parallel to IUL0203 and about 8 km to the southeast. It showed almost identical structural features but with better resolution.

The Nakhl Ophiolite block of the widespread Semail Ophiolite is overlain in the north by Tertiary sediments, and Quaternary alluvial deposits of the Tertiary Cover Sequence characterize the Coastal Zone. The top of the Hajar Supergroup could not be identified everywhere in the seismic reflection coverage of the Zone, probably because the thick Nakhl Ophiolite and the Tertiary Cover masks the Hajar Supergroup as seen in the Foreland. Chaotic seismic reflections to reflection-free zones were observed within the 2.5- to 10-km-thick Nakhl Ophiolite block (Shelton, 1990).

The Nakhl Ophiolite is exposed at the southwestern end of line IUL0205 adjacent to the northern limb of the Jebel Akhdar structure. The Ophiolite consists of both mantle and crustal units of the ophiolite body separated at the surface by a northward-dipping thrust boundary. The crustal section of the Nakhl Ophiolite has an average dip of about 20ºN (Nicolas et al., 1996). At the surface, a narrow exposure of the Hadhramout Group forms a distinct linear feature that dips in direction 15ºN. Line IUL0205 shows the upper boundary of the ophiolite body as dipping at about 25ºN based on the depth-converted section.

To the northwest of the transect, Hawasina Sediments overlie the volcanic section of the Semail Ophiolite. However, in the Coastal Zone, geological maps show no units equivalent to the Hawasina nappes as overlying the Nakhl Ophiolite block. Seismic lines IUL0203 and IUL0205 (Figure 3) provided no evidence of discordant units above the Nakhl Ophiolite. Three seismic stratigraphic sequences were identified as overlying the Nakhl Ophiolite block in Figure 10. They are as follows: (1) the Alkhawd Formation equivalent and the Hadhramout Group (late Campanian to Eocene); (2) the Asmari equivalent (Late Oligocene); and (3) the Lower Fars equivalent (Early Miocene to Recent).

On line IUL0205, the Alkhawd Formation equivalent is unconformable on the Nakhl Ophiolite. The Formation thickens toward the northeast and is pinched-out at the surface near the southwestern end of the seismic line. Cyclical shallow- to deep-shelf carbonates of the Hadhramout Group overlie the Alkhawd according to an unpublished 1985 report by Amoco Oman Petroleum Company. The base of the Hadhramout reflectors shows an ambiguous boundary relationship with the top of the Alkhawd that cannot be resolved without well penetrations. An Early Oligocene regional erosional unconformity recorded in well BA-1 (unpublished report, Amoco Oman Petroleum Company, 1985) marks a period of uplift that followed the deposition of the Hadhramout Group.

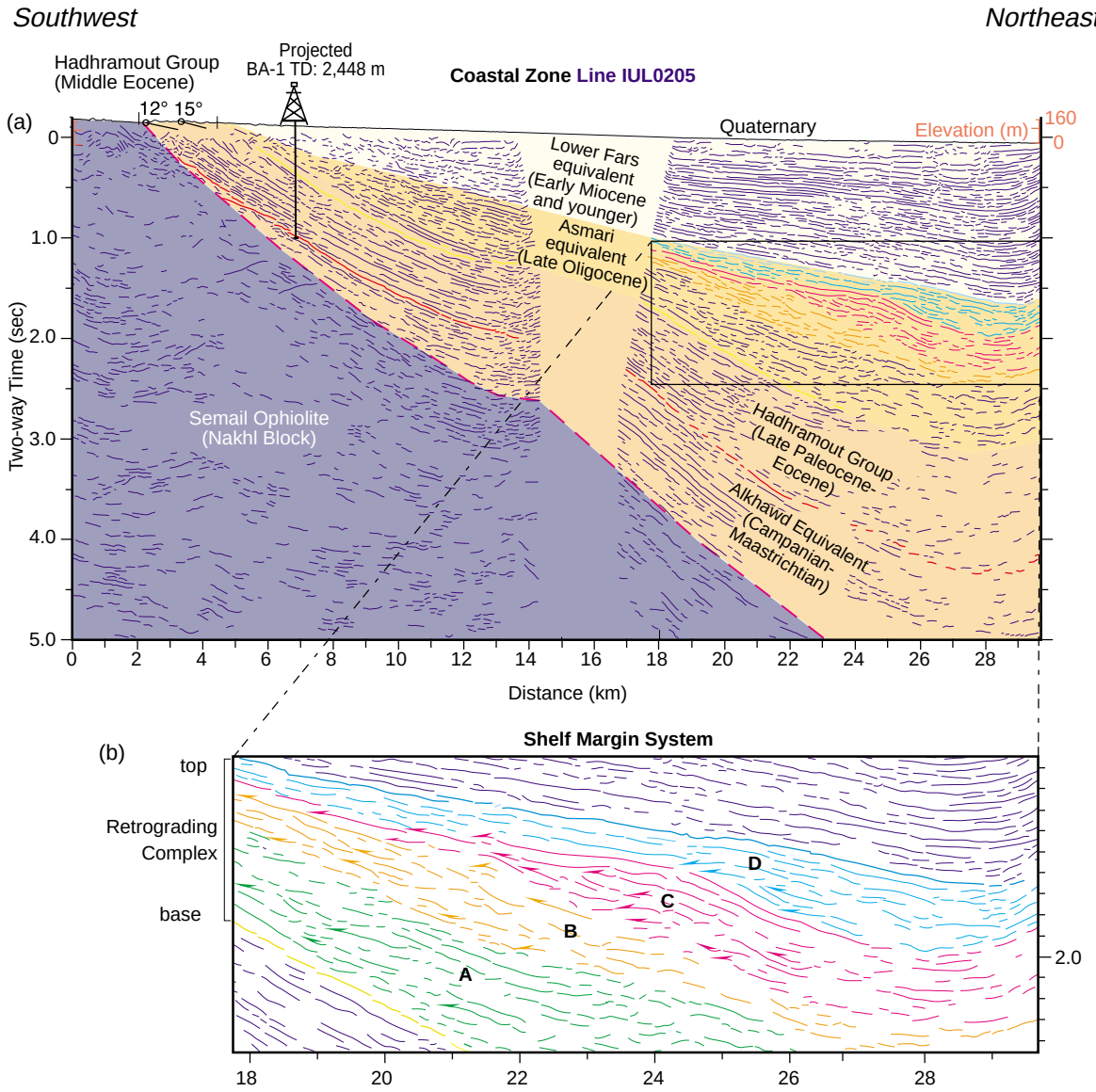

Figure 10: (a) Interpretation of 2-D seismic reflection profile of line IUL0205 showing the Semail Ophiolite (Nakhl Block) and the overlying stratigraphic units. (b) Seismic stratigraphy showing retrograding sequence complex along the continental shelf margin; A, B, C, and D are progradational sequences within the retrograding complex. The retrograding complex is indicative of episodic uplift of the Oman Mountains during the Oligocene. Note the seismic reflection gap between 14 and 16 km (for explanation see text below).

The interpretation of the seismic reflection data indicates a Middle to Late Oligocene marine transgression that led to the deposition of the Asmari Formation in a shallow outer shelf to marginal-marine environment (unpublished report, Amoco Oman Petroleum Company, 1985). Evidence from the seismic profile showed that the transgression was perturbed by episodic margin uplifts represented by the seaward migration of facies A, B, C, and D (inset Figure 10). Within each cycle, transgression is indicated by reflectors onlapping the top of the older cycle. The Lower Fars Group equivalent and the Quaternary alluvial deposits form a wedge-shaped seismic pattern, indicative of a continued margin uplift throughout the Miocene and possibly into Quaternary times.

The seismic reflection gap between 14 and 16 km is an offset of the NE-dipping Hadhramout Group that can be traced on seismic lines parallel to IUL0205 for about 45 km transverse to the transect. It may be due to a magmatic intrusion that was reported by Al-Harthy et al. (1991) to have occurred during the Tertiary on the northern flanks of the Jebel Akhdar and Saih Hatat structures.

MOHO DEPTH ESTIMATES FROM RECEIVER FUNCTIONS

Methods

Receiver function is a single-station teleseismic technique that employs the P-wave train to isolate structural effects at a seismic station. Generally, the receiver-function technique uses converted seismic phases, such as P to S (Ps) and converted P-wave multiples reflecting within the crust. For earthquakes at distances of more than 30º, seismic P-waves are steeply incident beneath a seismic station, and dominate the vertical components of ground motion. In contrast, a converted phase such as Ps, is largely contained in the horizontal components of ground motion (Clayton and Wiggins, 1976; Burdick and Langston, 1977; Cassidy, 1992; Zandt and Ammon, 1995; Sandvol, Seber, Calvert and Barazangi, 1998). The locally generated Ps phase amplitude is sensitive to the S-velocity structure beneath the station (Cassidy, 1992), and its arrival time relative to the first P-wave is used to estimate the depth of conversion. Since the largest velocity change in the lithosphere is along the Moho boundary, receiver functions are mainly used for Moho depth estimation (Sandvol, Seber, Calvert and Barazangi, 1998; Sandvol, Seber, Barazangi, et al., 1998).

A seismic wave propagating from a source to a seismic station includes information about the source mechanism, the velocity structure surrounding the source, the velocity structure along the ray path, and the crust and upper mantle structure below the recording station (Burdick and Langston, 1977). For the recording of teleseismic earthquakes, the converted Ps phase is isolated from the source effects by deconvolving the vertical component of ground motion with the radial components of the P-waveform to produce the time series known as Receiver Function (Zandt and Ammon, 1995). Whereas, the radial component is used to estimate Moho depth, the tangential component provides information about any possible dip in the Moho interface. Details of the receiver-function technique used are described in Sandvol, Seber, Calvert and Barazangi (1998) and will not be discussed further.

Table 1
Seismic station information, including recording days for each station as used in receiver function study.

Station Name	Latitude (N)	Longitude (E)	Elevation (m)	Recording time (days)
KTOM	23.48°	57.69°	107	142
AWBI	23.30°	57.53°	397	37
JBRN	22.91°	57.26°	552	43
BSYA	22.73°	57.24°	348	80

Data and Analysis

Teleseismic data were recorded by two short-period (1 Hz), 3-component, portable digital instruments deployed at four locations (stations KTOM, AWBI, JBRN, and BSYA) on the transect (Figure 3). The stations were at locations where electrical power was available and accessibility to the site was not restricted and each was occupied for at least two months, (Table 1). The sampling interval was 50 samples per second.

The recorded teleseismic earthquakes were mainly from events in the western Pacific (Japan, Philippines, Taiwan, Papua New Guinea, and Indonesia) (Figure 11), and most were associated with subduction zones. They provided the necessary distance required for receiver-function analysis. We used the time difference between the primary P-wave arrival and the converted P to S-wave (Ps) arrivals (Figure 12) to estimate depth-to-Moho along the transect. The average time differences between Ps-Moho and P are 4.7, 5.6, and 4.9 seconds for the stations KTOM, AWBI, and JBRN, respectively (Figure 12). We observed no obvious converted Moho phase (Ps-Moho), at station BSYA, possibly due

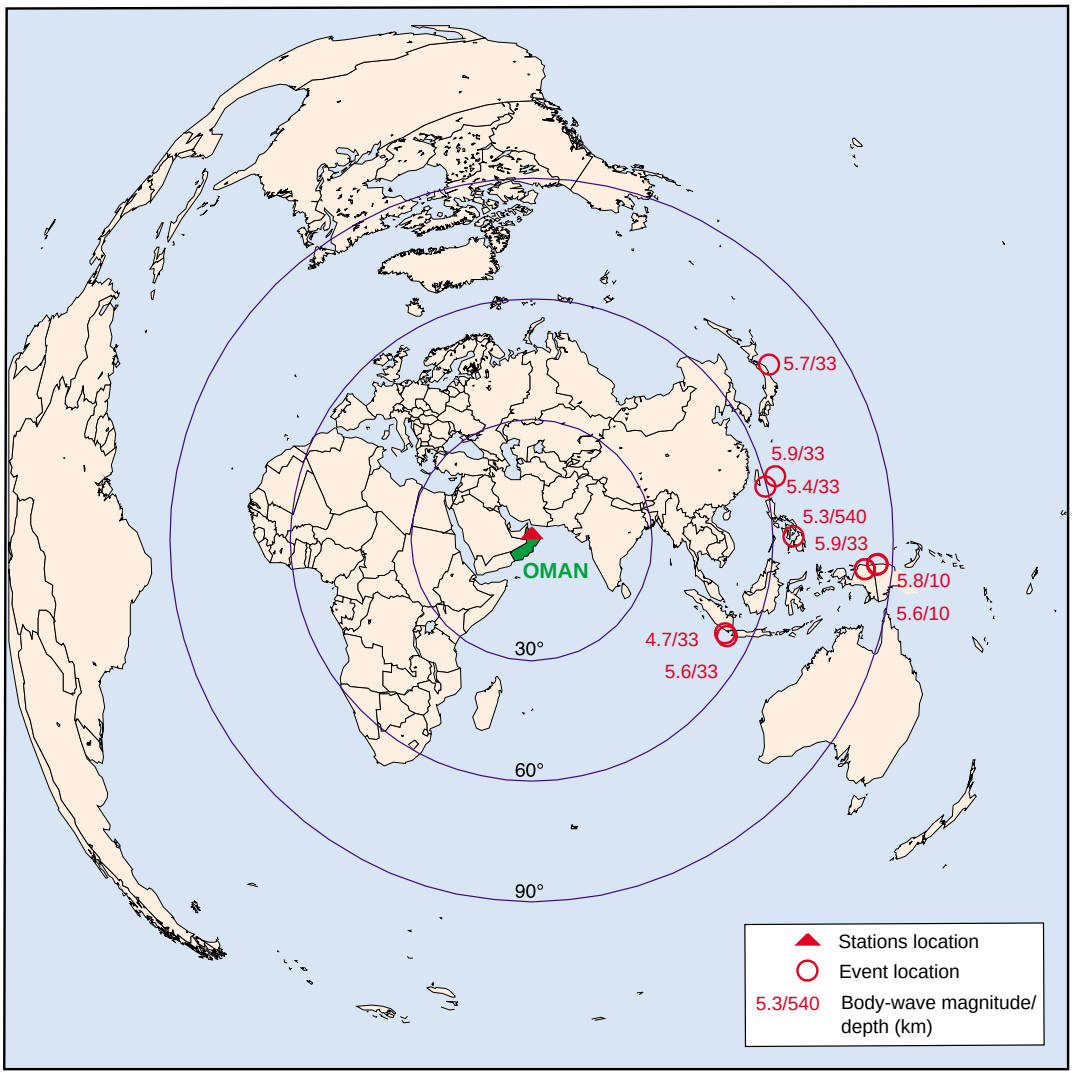

Figure 11: Locations of teleseismic earthquakes that were used to obtain the final receiver function response for stations KTOM, AWBI, JBRN, and BSYA (see Figure 3 for location of stations). Recorded events location, magnitude, and depth information were obtained from the US Geological Survey Earthquake Event Catalog.

to site problems. The receiver function of station KTOM gave the clearest signal that exceeded the noise level. At all stations, the tangential components of the receiver function gave no indication of a steeply dipping Moho, as shown by the low amplitudes in the tangential component at the arrival times of the Ps phase. From our analysis of the receiver functions, we observed an intracrustal phase conversion (Ps-crust) beneath stations JBRN and BSYA.

In order to estimate the depth-to-Moho using the receiver functions shown in Figure 12, accurate velocity information beneath each station was required. We did not have information on the average crustal velocity from directly beneath the stations, but studies of the eastern Arabian Shield had estimated the average P-wave velocity of the crust in the region to be 6.6 km / sec (Mooney et al., 1985) and 6.5 km / sec (Badri, 1990).

These values were considered to be representative of the eastern Arabian margin and Foreland. However, the study area has significant thickness of sediment that could affect the average crustal velocities. To estimate the effect of the sedimentary section, we used the average sonic velocity for the total depth of wells DA-7 and ML-1. The average velocity for the approximately 5-km-thick sedimentary section was between 5.2 km / sec and 5.4 km / sec (Figure 4). In this region, sedimentary units younger

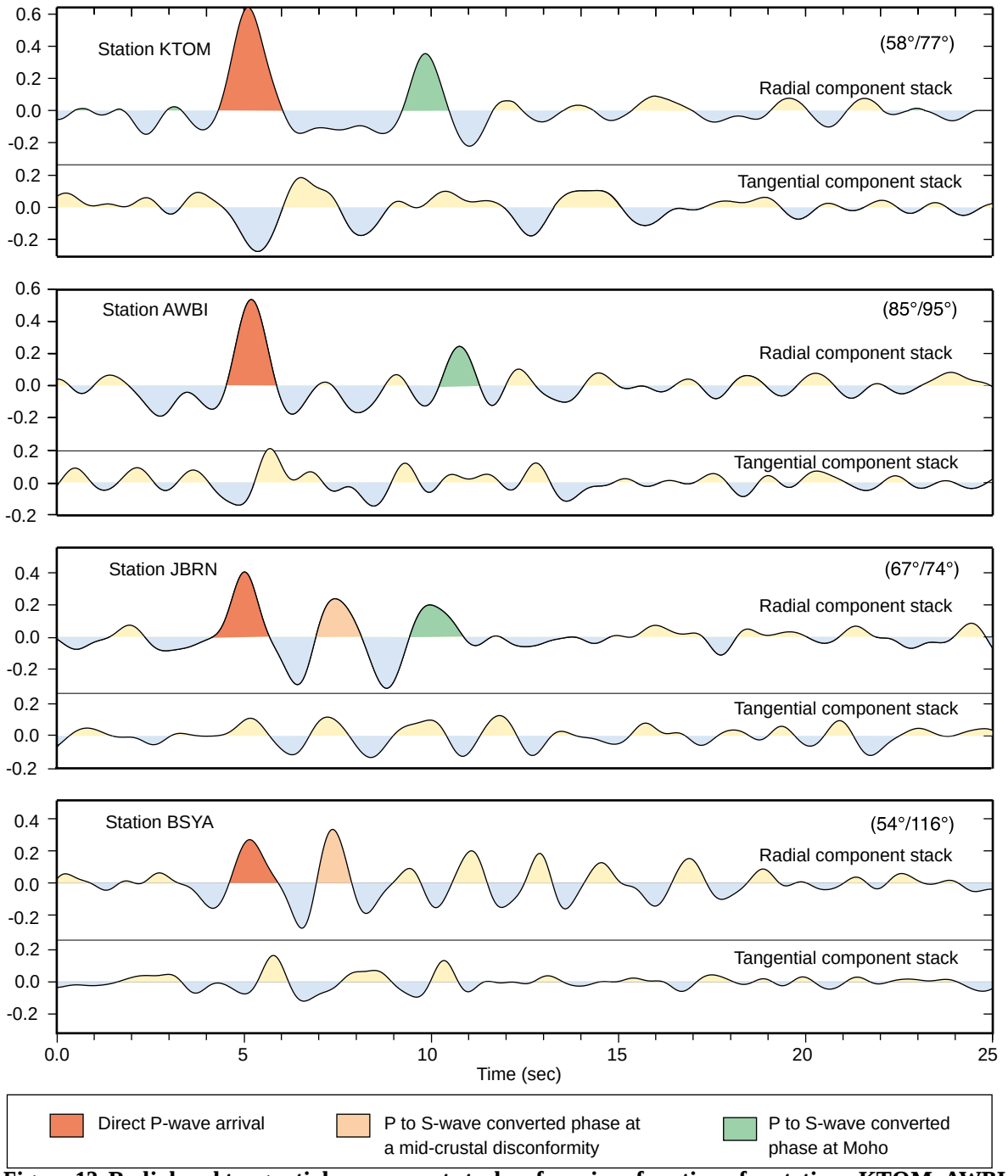

Figure 12: Radial and tangential component stacks of receiver functions for stations KTOM, AWBI and JBRN, BSYA. Values in brackets denote distance between station and event/back azimuthal direction from station to event.

than Late Cretaceous have an average velocity of 3 km / sec. The thickness of the post-Late Cretaceous sediments varies, but the maximum thickness along the transect is only from 1 to 1.5 km and this would have an effect of about 2 percent on the averaged crustal velocity.

Since we did not have absolute velocity values for the entire crust and only average measurements from a nearby region, we used a range of velocity values (minimum 6.4 km / sec, maximum 6.8 km / sec) for the whole crust to take into account any potential uncertainty. An additional velocity error is introduced by the converted phase (Ps) wavelength where the interface resolution is dependent on the frequency of the impinging wave. Hence, we estimated an additional error of about 1 km.

Results (Figure 13)

Station KTOM

Based on a 6.6 km / sec crustal velocity, and a 0.25 Poisson ratio (Zandt and Ammon, 1995), the calculated Moho depth for station KTOM on the southern edge of the Coastal Zone was 41 km. Taking into account potential errors, we estimated the Moho depth beneath this station to be 41 ± 2 km. Due to the incident angle of the incoming seismic wave, the actual Moho impingement is at 8 km east of KTOM (see Figure 3) based on the assumed seismic velocity.

In the Coastal Zone, the ophiolite blocks are estimated to vary in thickness from between 10 and 20 km (Shelton, 1990). Ophiolites in northern Oman have an average compressional velocity of about 6.9 km / sec (Christensen and Smewing, 1981) and account for at least 25 percent of the average continental crust thickness of 45 km in the region. This high velocity could result in a decrease of about 4 km in the estimated Moho depth at station KTOM, which is approximately equal to the total estimated error.

Station AWBI

This station recorded a depth-to-Moho of 49 ± 2 km, which is about 8 km deeper than at KTOM. The impingement location of station AWBI (see Figure 3) is within the northern limb of the Jebel Akhdar range, which isolates it from the high-velocity ophiolite effect of the region.

Station JBRN

A Moho depth of 43 ± 2 km was calculated for this station on the southern side of the Jebel Akhdar range. The actual Moho impingement of JBRN (see Figure 3) is within the Hamrat Ad Duru Zone where the ophiolite body is only about 500 m thick (based on seismic and gravity modeling). As such, the ophiolite would not have any significant effect on the calculated depth.

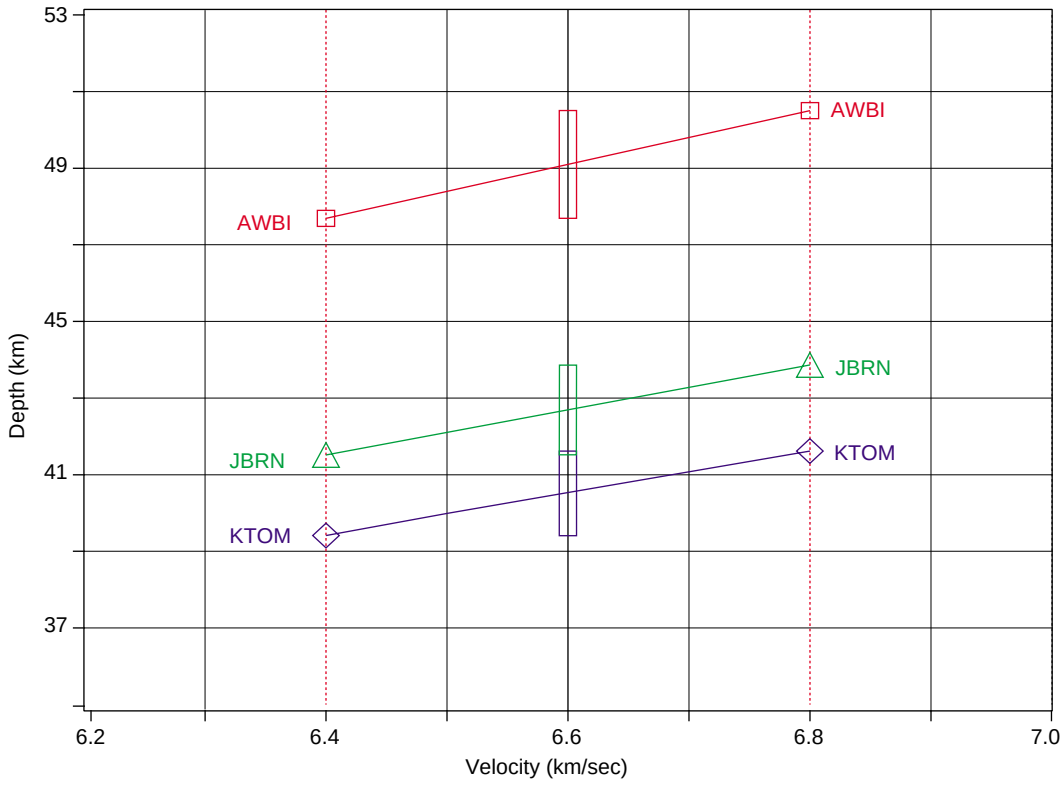

Figure 13: Velocity-depth trade-off curves for stations KTOM, JBRN and AWBI. For a 6.6 km/sec average crustal velocity, we estimated a Moho depth of 41 ± 1 km, 43 ± 1 km, and 49 ± 1km for stations KTOM, JBRN, and AWBI, respectively. The depth error bar was estimated for a velocity minimum of 6.4 km/sec and maximum of 6.8 km/sec velocity error.

No Moho depth estimate was made at Station BSYA as no obvious converted Moho phase (Ps-Moho) was observed, possibly due to site problems.

GRAVITY MODELING

In order to determine the subsurface structure along the entire transect, we used gravity modeling that was constrained by the existing seismic reflection profiles, well logs, and receiver function results. Gravity modeling provided data that was unavailable from the seismic profiles and well logs.

The seismic and well log data gave thickness information for the upper 8 km along the transect, excluding the Jebel Akhdar range that has no seismic coverage or wells. However, seismic reflection profiles alone could not provide the total depth-to-basement. Similarly, the receiver function provided accurate Moho depths at three points on the transect but could not predict the Moho topography elsewhere.

Gravity modeling is a non-unique technique but our use of seismic, well logs, and receiver-function results improved its usefulness. A GMSYS gravity modeling software package from Northwest Geophysical Associates Incorporated was employed. It uses a 2.5-D body model that allows limits to be placed on the lateral extent of each modeled body.

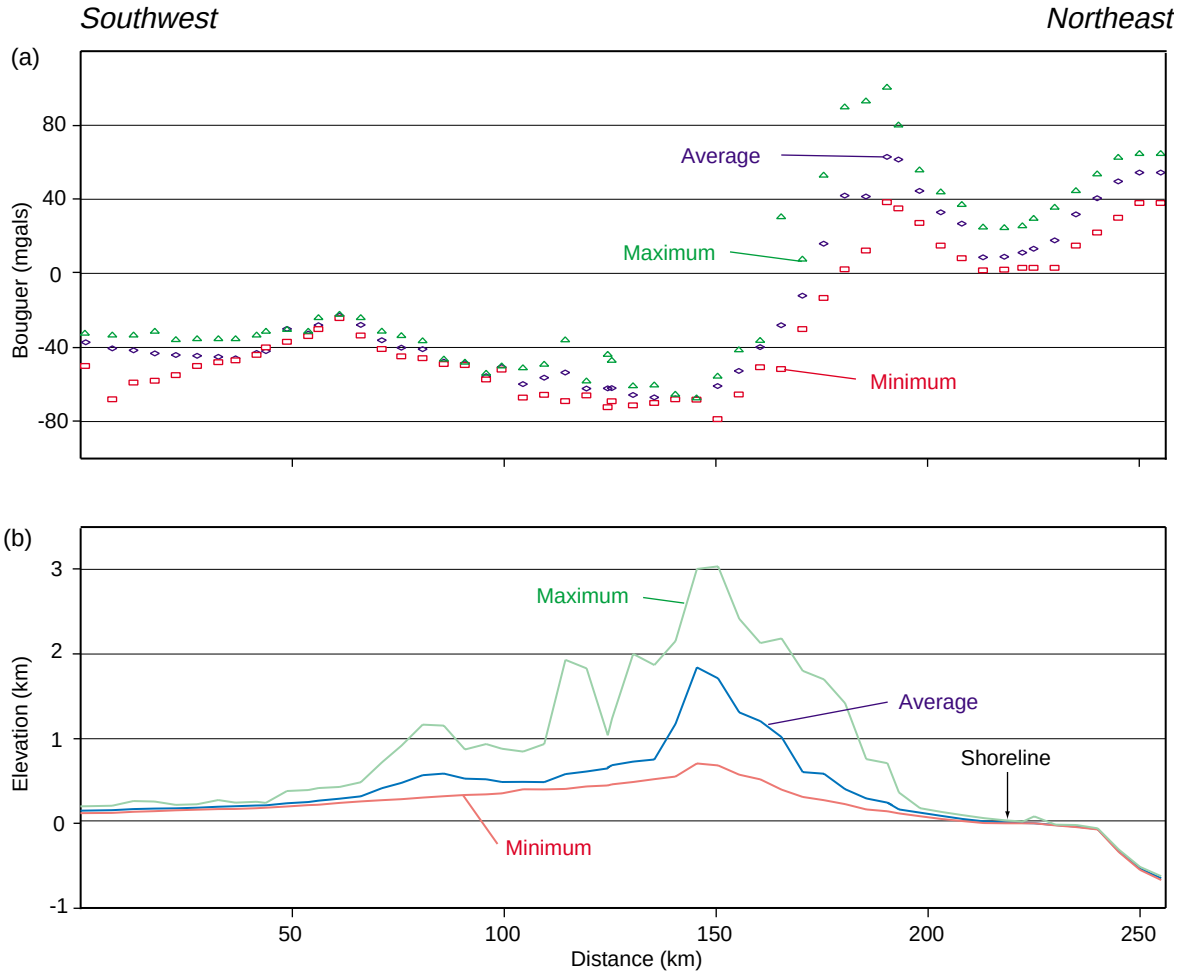

Figure 14: (a) Plot of maximum, minimum, and average Bouguer gravity anomalies in a 50-km-wide swath along the transect (see Figure 3 for location). (b) Plot of maximum, average, and minimum elevation profiles along the transect. Gravity and elevation values were calculated for a 5-km sampling interval along the entire transect.

Data

In our study, we used the Bouguer gravity data for Oman compiled by Ravaut and Warsi (1997). The Bouguer gravity anomalies are based on internationally accepted gravity formulae and were corrected for a slab of density 2.67 g/cc. The Bouguer point values and surface elevation data at 5-km intervals were taken from a 50-km-wide swath along the transect. In areas where there was no digital information, we obtained the average Bouguer values from the published Bouguer Anomaly Map of Oman by Ravaut and Warsi (1997) with the same sampling interval and swath width. Figure 14 is a plot of the average gravity and altitude values. Density information of modeled stratigraphic units was primarily obtained from corrected bulk density values and/or transient sonic velocity from well logs. Transient sonic velocity values were converted to density values by means of Gardner's equation (Gardner et al., 1974).

Wells JKH-2, FH-1, and SD-1 provided density values for the Hawasina Sediments (2.45 g/cc) and the Aruma Group (2.28 g/cc). Values for the Hajar Supergroup (2.6 g/cc) were obtained from wells ML-1 and DA-7 located northwest of the transect (see Figure 3), and those for the ophiolite (3.07 g/cc) and the upper mantle (3.3 g/cc) were taken from a previous study by Ravaut (1997a) in the region. We estimated the pre-Permian Sequence density to be from 2.5 to 2.55 g/cc in order to accommodate the Ara salt of 2.2 g/cc. The salt is present throughout the study area, and has an enormous thickness variation of from zero to 2,000 m (Mattes and Morris, 1990; Mount et al., 1998). Our estimated pre-Permian Sequence density made a good model fit with the observed gravity values (Figure 15). We estimated a comparable density for the middle and lower crust of 2.7 g/cc.

Constraints on the data interpretation in the Coastal Zone included the upper boundary of the ophiolite block that dips north at 25º, and the density of the ophiolite and of the overlying sequences. Well BA-1 provided density information for the Hadhramout Group (2.45 g/cc) and for the Eocene-Holocene sediments (2.2 g/cc). In the Coastal Zone, we estimated the density of the Alkhawd Formation equivalent to be the same as that of the Hadhramout Group. In this Zone, the edge of the continental margin was found to be about 40 km northeast of the end of the transect where it drops off into the Oman remnant basin at about 3,000 m depth. Therefore, we allowed for the termination of the shelf and the pre-Permian Sequences toward the northeastern end of the model (Figure 15) and for the depth-to-basement to shallow in the same direction.

Moho depths obtained at stations KTOM, AWBI, and JBRN were used to constrain the structure of the Moho across the Jebel Akhdar range. In all models, we allowed the Moho depth south of Jebel Akhdar to vary about the determined Moho depth of 43 km at JBRN. Toward the northeastern end of the transect, we varied the Moho depth below what was obtained at KTOM in order to accommodate crustal thinning toward the oceanic Gulf of Oman. In addition, we allowed the Moho depth to vary beneath Jebel Akhdar so as to take into account possible crustal thickening.

Observed Bouguer gravity values along the transect varied from -80 mgal beneath the Jebel Akhdar range to a maximum of+100 mgal about 40 km to the northeast (Figure 14). In the Foreland region of the southwest, the values are uniform at about -40 mgal with a variation of about 20 mgal. The values decrease northeastward and reach their minimum at Jebel Akhdar. From this point northward, the Bouguer gravity values increase sharply toward the continental margin. A shorter wavelength positive anomaly is superimposed on the regional anomaly, northeast of Jebel Akhdar at about 180 km. This anomaly corresponds to the Nakhl Ophiolite block. Farther north, the anomaly increases to an average value of + 60 mgal reflecting crustal thinning and the proximity to the oceanic crust of the Gulf of Oman. A superimposed negative anomaly at about 225 km coupled with the positive ophiolite anomaly corresponds to a small intramargin basin.

The ophiolite emplacement in the Oman Mountains resulted in variable grades of metamorphism (El-Shazly and Coleman, 1990). Amphibolites and greenschists were formed in the high-temperature, low-pressure environments at the base of the ophiolite, whereas high-pressure, low temperature eclogites and blueschist facies occurred at various levels within the Hajar Supergroup and the pre-Permian sequence along the continental margin. High-pressure, high-temperature conditions were restricted to the Saih Hatat structure with the formation of eclogites on its northern boundary

(El-Shazly and Coleman, 1990). In contrast, the Jebel Akhdar structure was affected only by the early phases of well-developed cleavage deformation (Le Métour, Bechennec and Roger, 1995). To accommodate this low metamorphic gradient we included a density increase toward the northeast across Jebel Akhdar to the Coastal Zone. The low-density gradient increase affected lithologic units overlain by the Hawasina Sediments and the Semail Ophiolite.

Gravity Analysis

Model-A

In general, basement topography in the Foreland region was found to mimic the observed gravity response (Figure 15, Model A). Gravity modeling showed a relative basement high at a depth of about 7 km below the Jebel Qusaybah structure. The relative anomaly is part of a basement high at an average depth of 9 km that extends for about 60 km from the Maradi Fault Zone to the center of the Hamrat Ad Duru Zone. Basement depths south of the Maradi Fault Zone and the northern end of the Hamrat Ad Duru Zone average 13 km. A small anomaly of less than 10 mgals corresponded to the ophiolite body directly south of Jebel Akhdar. The depth to the basement in the core of Jebel Akhdar was about 9 km and this implied a thickened pre-Permian Sequence below the Jebel Akhdar range (Figure 15).

The considerably thickened pre-Permian Sequence at the core of Jebel Akhdar corresponded to a short wavelength gravity response that could not be compensated by depth changes at the mountain root. The northern limb of Jebel Akhdar, however, showed an extensively thinned pre-Permian Sequence below the Allochthonous Sequence of the Semail Ophiolite and the Hawasina Sediments. North of Jebel Akhdar, a positive and a negative anomaly couple overrode the regional anomaly and corresponded to the N-dipping ophiolite body and the intramarginal Tertiary basin, respectively. The average thickness of the ophiolite block north of Jebel Akhdar was interpreted to be 5 km with a lateral extent of about 95 km to the north.

Below the ophiolite, the Hawasina Sediments have an average thickness to about 1 km along the Coastal Zone, but thicken to approximately 4 km below the outcrop of the ophiolite block directly north of Jebel Akhdar (Figure 15). Based on Model-A, the modeled Hawasina Sediments north of Jebel Akhdar are comparable in thickness to those south of Jebel Akhdar that were constrained by seismic and well data. The geometry of the ophiolite body in all models required a leading and a trailing wedge of variable density and a thickness of between 5 and 8 km. The depth-to-basement in the Coastal Zone reached its maximum at about 17 km below the outcrop of the ophiolite body. It shallowed northeastward and imposed thinning of the Hajar Supergroup and the pre-Permian Sequence (Figure 15).

Model-B

In this model, we included a semi-gradual density increase of 0.05 g/cc from southwest to northeast for the pre-Permian Sequence, the Hajar Supergroup, the Hawasina Sediments, and the Aruma Group (Figure 15). Because the density of the pre-Permian Sequence was increased to 2.55 g/cc, the depth-to-basement was reduced by about 2.5 km in the Interior and Hamrat Ad Duru zones and the thickness of the pre-Permian Sequence was correspondingly reduced. Consequently, only large topographical differences, such as the Jebel Qusaybah anomaly, were clearly resolved in the Foreland region. North of the Mountain and Coastal zones, this density change resulted in a dip increase of the northern limb of the Jebel Akhdar range (Figure 15). This consequently increased the thickness of the Hawasina Sediments at the expense of the ophiolite body. Thickness-density trade-offs between the Hawasina Sediments and the ophiolite resulted in an irregular ophiolite body that we did not consider as being the favored model. To further constrain the model in the Coastal Zone, we require information on the extent of the Hajar Supergroup and pre-Permian Sequence beneath the ophiolite body, or the thickness of the ophiolite and density values for the lower and middle crust.

Model-A (Figure 15) is our favored model, but Model-B is an alternative and provides an error estimate for the preferred model.

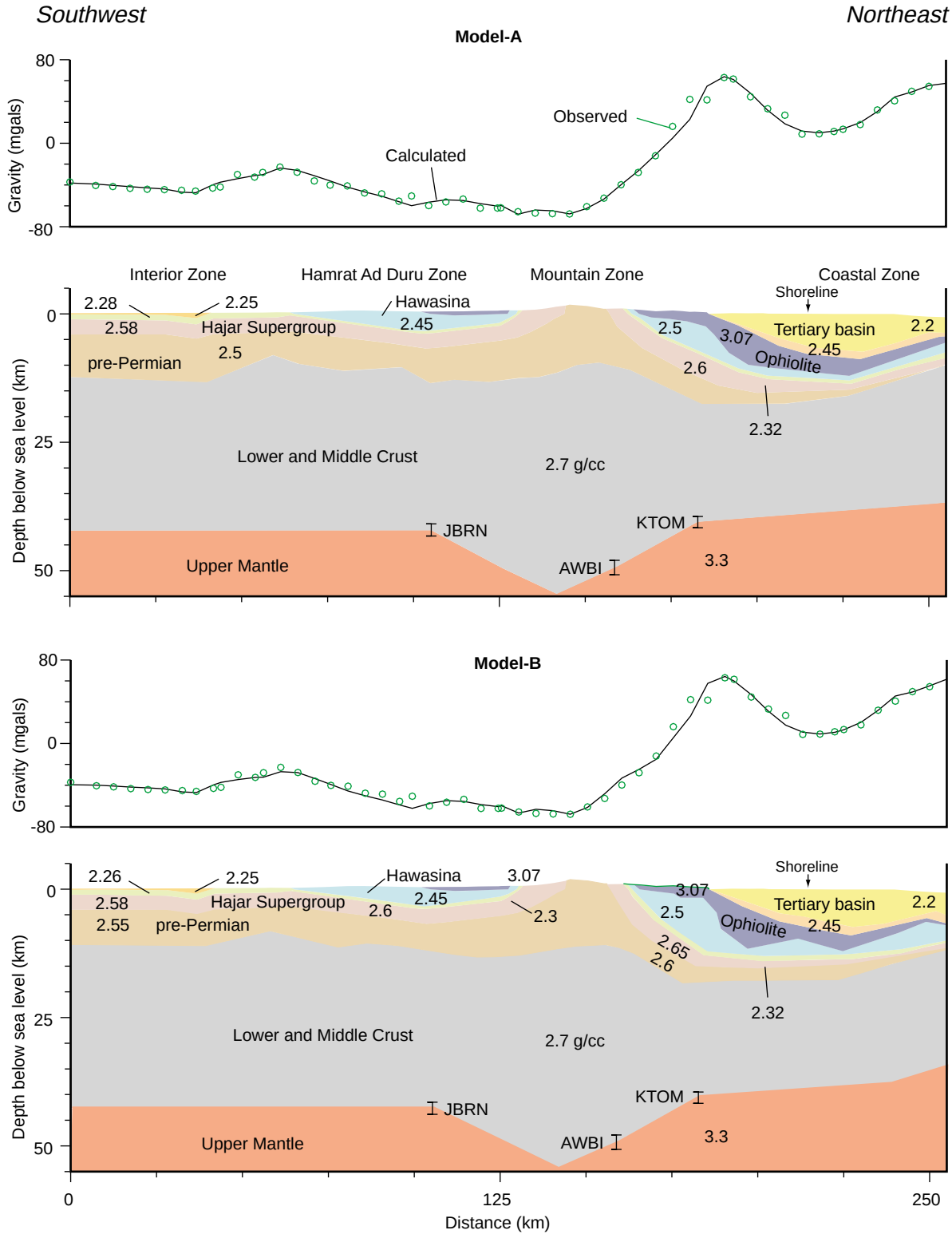

Figure 15: Cross sections of the crust and upper mantle obtained from gravity modeling. Model-A: density values of 2.7 g/cc and 2.5 g/cc for the lower crust and the pre-Permian Sequence, respectively. A minimum lateral density variation is allowed in this model. Model-B: density values of 2.7 g/cc and 2.55 g/cc for the lower crust and the pre-Permian Sequence, respectively, allowing relatively more lateral variation in density values along the transect. Density values increase from southwest to northeast in both models. Moho impingement from seismic stations JBRN, AWBI, and KTOM is shown by error bars.

DISCUSSION

Compilation of multidisciplinary results based on seismic reflection, well data, receiver-function analysis, and gravity modeling, together with surface geology, provided reliable constraints for the construction of a complete crustal transect across the Foreland region, the Mountain Zone, and the Coastal Zone (Figure 16). Furthermore, data analysis and interpretation provided structural and stratigraphic relationships that added to the understanding of processes that accompanied the emplacement of the Semail Ophiolite and later developments along the continental margin and in the Foreland region.

Foreland Region

Authors such as Robertson (1987), Boote et al. (1990), and Bechennec et al. (1995), have collectively summarized the nature of the emplacement of the Semail Ophiolite on the Arabian continental margin and in the Foreland region. They proposed that three distinct evolutionary processes had taken place; they were: (1) doming; (2) complete margin subsidence; and (3) the final subsidence of the Foreland during and after ophiolite advancement.

Based on the interpretation of seismic lines S50295 (Figure 6) and R41019 (Figure 9)—and others in the Foreland region not shown on Figure 3—we concluded that our interpretation of the seismic stratigraphy conforms well to the three events, as follows:

(1) Doming during the Turonian was marked by an erosional unconformity at the top of Natih Formation (Albian) throughout the Foreland region (Bechennec et al., 1995). We observed that relatively more erosion at the top of Natih Formation had affected the Hamrat Ad Duru Zone and the Fahud area (well FD-1) (Figure 5).

(2) In the second stage of emplacement, complete margin subsidence resulted in the development of the Muti basin throughout the Foreland region and the Mountain Zone (Robertson, 1987; Boote et al., 1990; Bechennec et al., 1995). As an indication of regional subsidence, the Turonian-Santonian Muti Formation (as interpreted from the seismic stratigraphy), overlies the Natih Formation throughout the Foreland region (Figures 7, 8, and 9).

(3) The third stage of the emplacement was the advancement inland of the Allochthonous Sequence across the continental margin, as marked by the development of the extensive Campanian-Maastrichtian Fiqa basin (Bechennec et al., 1995). The Fiqa Formation records the stratigraphic interaction as the allochthonous body progressed toward the Foreland (Figures 6 and 9). Southerly prograding reflectors of the Fiqa Formation are interpreted as downlapping the top of the Muti Formation and being indicative of a localized topographic high moving southward (Figures 6 and 9) due to the southward migration of the peripheral emplacement bulge of the Semail Ophiolite. The prograding reflectors onlap the southwestern edge of the Fahud area in the Interior Zone where it is possible that the southerly movement of the peripheral bulge ceased (Figure 6). Our observations conform to those of Robertson (1987) whereas they conflict with Warbuton et al. (1990) who advocated a non-migrating peripheral bulge. As the peripheral bulge advanced, the region became a deep, open marine, outer shelf to upper bathyal environment in which the Fiqa Formation was deposited (Robertson, 1987; Bechennec et al., 1995).

The formation of the Jebel Qusaybah anticline is thought to have occurred during Santonian time. This is in agreement with Hanna and Smewing (1996) who show that growth of the Jebel Salakh structure began in the Late Cretaceous during deposition of the Aruma Group. In Figure 8, the Muti Formation and Hajar Supergroup are both folded and indicate that deformation postdated deposition of the Muti. In addition, reflectors of the Fiqa Formation onlap the southern side of the Jebel Qusaybah anticline (Figure 8). Reflectors below the Hajar Supergroup at about 2.0 sec (TWT), show no conclusive evidence of either folding or faulting that would infer a salt-supported structure.

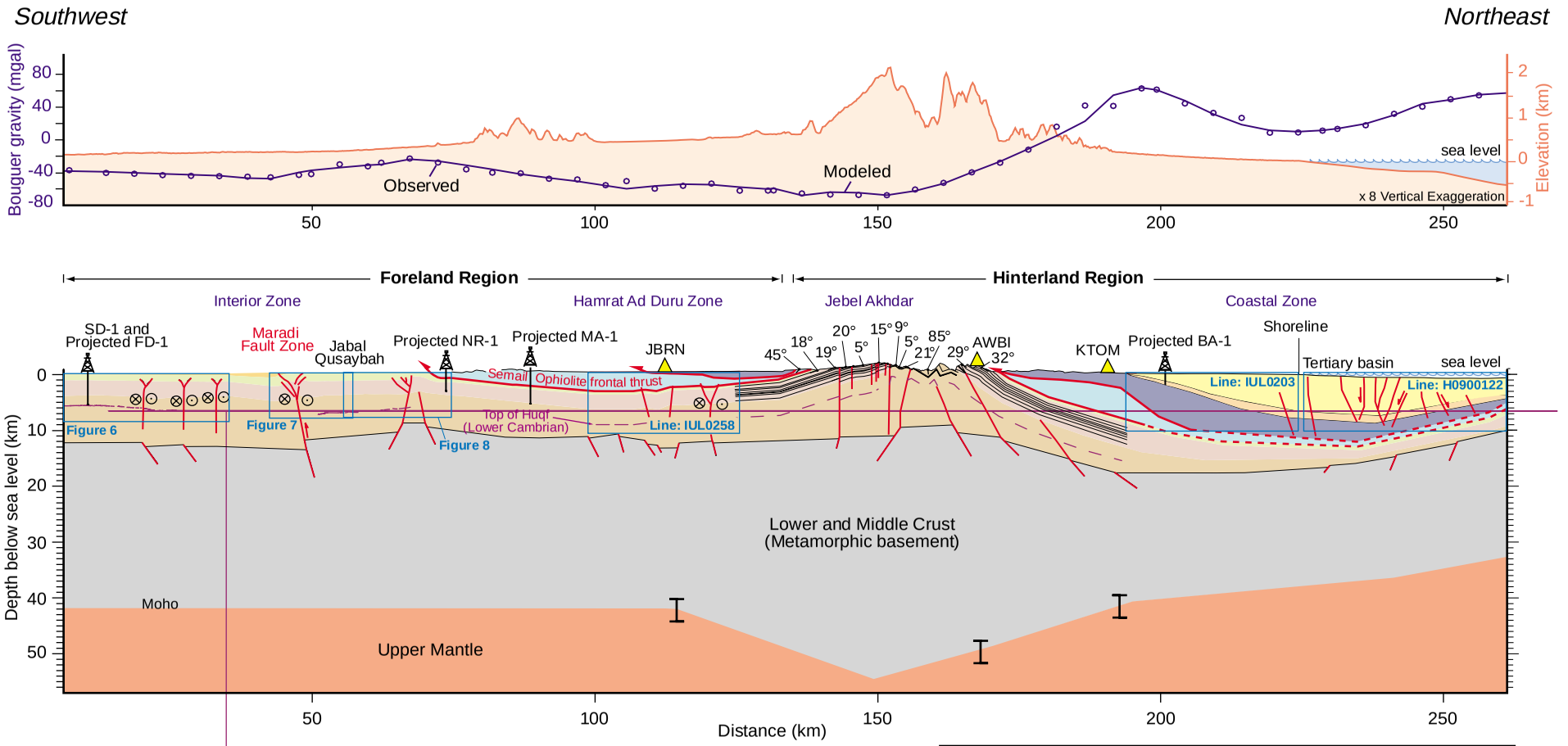

Figure 16: The entire transect of the crust and parts of the upper mantle from the Hinterland in the northeast, across the Jebel Akhdar range, and into Interior Oman in the southwest, together with the observed and model Bouguer gravity values and the corresponding ground elevation. Important stratigraphic sequences and formations, and structural relations are shown. Faults are in red, and a bold red line delineates the Semail Ophiolite frontal thrust and the sole of the Hawasina Sediments. Dip information is given in the Jebel Akhdar range. Deployed seismic stations are shown as yellow triangles with corresponding, projected Moho impingement locations as error bars. Wrench faults: away from observer ⊗; toward observer ⊙.

.

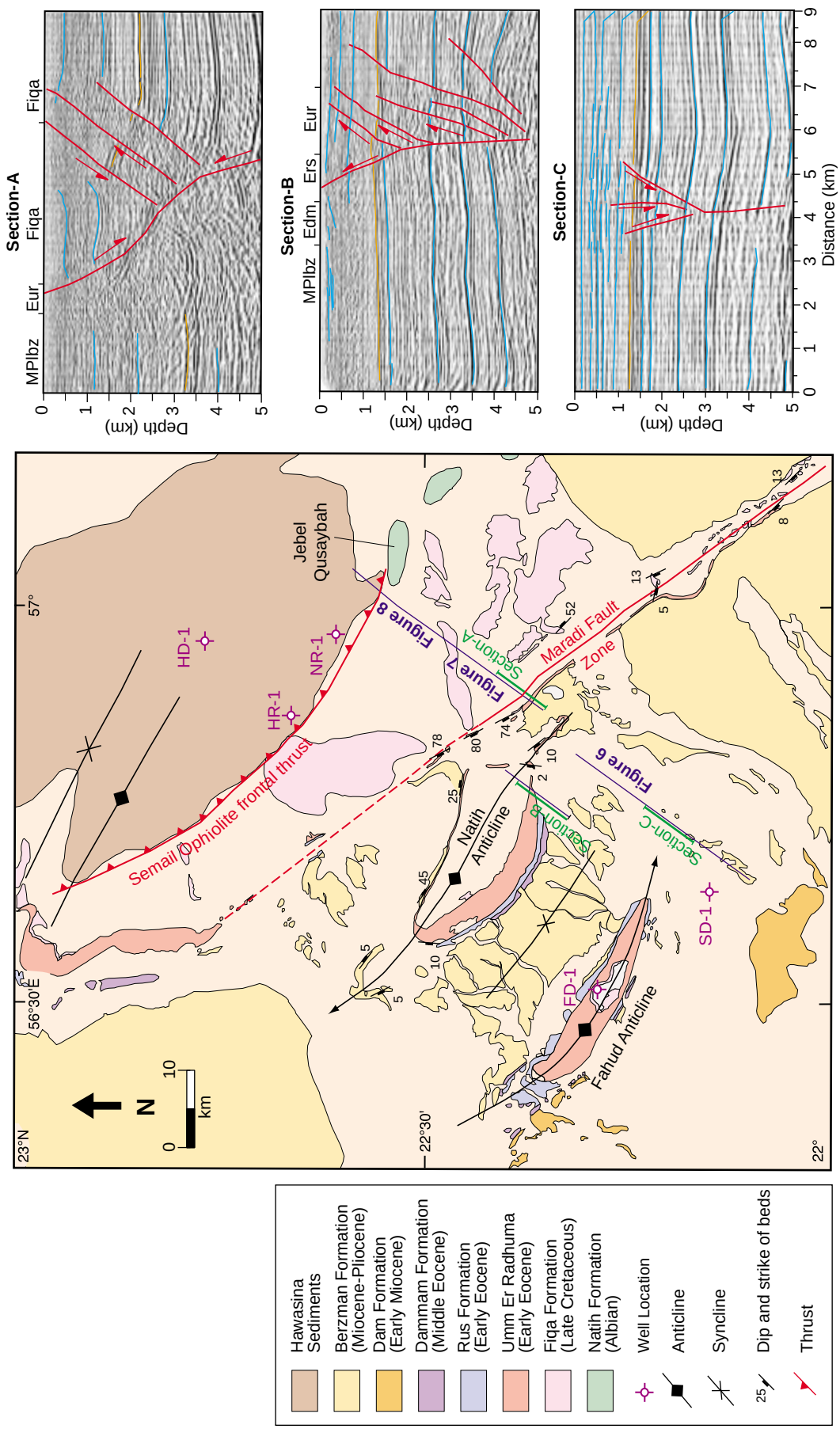

Figure 17: Geologic map of part of the Foreland region (see Figure 3 for location); extracted from 1:250,000-scale Geological Maps of Oman (1992). The depth-converted sections (A, B, and C) are shown without vertical exaggeration. They were used to infer subsurface structural relationships between the Maradi Fault Zone, Natih and Fahud structures and a NW-trending wrench-fault system, seen as flower structures in each section; red lines denote faults; random reflectors are colored blue to enhance the structure. Flower structures in Section-A and Section-B are positive, whereas in Section-C the flower structure is negative. Eur = Umm Er Radhuma; Ers = Rus Formation; Edm = Dammam Formation; MPlbz = Berzman Formation.

Farther east, the Maradi Fault Zone acted as a barrier, so that wells NR-1 and HR-1, located north of the fault zone show no deposits of the Lower Eocene-Pliocene Hadhramout or the Fars Group of the Tertiary Cover Sequence (see Figures 5 and 17). Also, to the northeast of the fault zone, the top of Hajar Supergroup is about 900 m higher relative to the southwestern side of the fault. The absence of the Tertiary cover northeast of the Maradi Fault Zone could be the result of differential uplift or differential subsidence. In the case of uplift, the Tertiary cover was removed by erosion in the higher northeastern area, whereas in the case of differential subsidence, the Tertiary rocks were not deposited at all to the northeast of the fault zone. Based on our observations, we interpreted the Maradi Fault Zone to be a basement-associated fault having two styles of deformation. The two styles were (1) a reverse faulting component as a pre-Maradi Fault Zone (possibly occurring early in the Late Cretaceous), and (2) a strike-slip fault component dated as a Pliocene-Pliestocene event by Hanna and Nolan (1989) (see Figures 7 and 17).

Observations of various seismic profiles (some of which are not included on Figure 3), consistently showed flower structures in a NW-trending wrench fault system. The structures affected the entire Hajar Supergroup, the Muti Formation, and the Aruma Group in the Interior and Hamrat Ad Duru zones (Figures 6, 7, and 8). In most seismic profiles, the flower structure offsets can be traced within the overlying Muti and Fiqa formations; however, in some cases faulting within the Fiqa becomes ambiguous as in Figure 6.

In our study, we interpreted the Fahud and Natih anticlines as periclines possibly associated with strike-slip movement along the already weakened zone of the pre-Maradi Fault Zone. The two structures have a difference in strike of about 20º with respect to the fault zone (Figure 17). The fault zone is parallel to the system of NW-trending wrench faults that was seen on seismic lines throughout the Foreland region and which implies a regional, possibly transcurrent, event. In Figure 17, Section-B intersects a positive flower structure at the southeastern end of the Natih structure. As seen on the accompanying geologic map, the deformation of the Natih and Fahud structures includes the Miocene-Pliocene Berzman Formation that overlies the Hadhramout group. The timing of this event is in agreement with earlier work by Hanna and Nolan (1989) who dated the Maradi Fault Zone as a reactivated Pliocene-Pliestocene right-lateral strike-slip fault. We suggest that the Tertiary deformation in the Foreland region was largely transcurrent with no conclusive evidence of a major compressional event (Figure 17).

Hinterland Region

Three important questions have been posed regarding the present-day Jebel Akhdar and the Oman Mountains.

(1) What is the support mechanism for the present-day topography?
(2) What type of structural style is involved in the architectural formation of Jebel Akhdar, and what was its timing?
(3) What was the timing of uplift of the Oman Mountains?

In the discussion below, we conclusively answer (1) and propose a solution for (3). We are not able to provide a specific solution for (2) as it requires more detailed structural analysis and deeper seismic imaging, but we do propose a mechanism for the formation of the Jebel Akhdar range.

Answering question 1, Moho depths determined from data obtained from seismic stations JBRN, AWBI, and KTOM delineated the root beneath the Jebel Akhdar range, and this was confirmed by gravity modeling. However, station AWBI, which gave the deepest Moho values (48–51 km) of the three locations, does not correspond to the highest elevation of Jebel Akhdar. As shown in Figure 16, the coincidence of the highest point in the topography with the lowest gravity point is 10 km southwest of AWBI. Assuming an isostatically compensated Airy model, the highest elevation (3,000 m), would correspond to a Moho depth of about 55 km (Figure 16). The gravity modeling results of Manghnani and Coleman (1981) and Ravaut et al. (1997) gave maximum Moho depths below Jebel Akhdar of about 43 km and 47 km, respectively, which is shallower than the depth interpreted beneath station AWBI. Both Manghnani and Coleman (1981) and Ravaut et al. (1997) used an average density of

2.9 g/cc for the continental crust, which we found to be too high. Our gravity modeling also differed by including more constraints on the upper 8 km of the sedimentary section, and included Moho depths across Jebel Akhdar interpreted from new seismological observations.

We associate the beginning of crustal thickening below the Jebel Akhdar range to the Late Cretaceous emplacement of the Semail Ophiolite and its large southward-directed compressional component.

With regard to question 2, two styles of deformation have been proposed in relation to the present-day Jebel Akhdar. They are a fault-bend fold (Michard et al., 1984; Cawood et al., 1990; Hanna, 1990), and a propagation-fault fold (Mount et al., 1998). We interpret the present-day structure of Jebel Akhdar as deformation concentrated along zones of weakness, perhaps shear zones, related to the Permian rifting event. We infer the initiation of the Jebel Akhdar structure to be contemporaneous with the third stage of the Semail Ophiolite emplacement, when the allochthonous load had collided with the edge of the continental margin. Nolan et al. (1990) concluded that the Alkhawd Formation mapped on the flanks of Jebel Nakhl and Saih Hatat included clasts that recorded the unroofing and erosion of the Saih Hatat and Jebel Akhdar culmination. The timing of the event was deduced from observations described below.

Gravity modeling showed that the top of the basement in the core of the Jebel Akhdar structure is at about 9 km depth, and that it coincides with the extensively deformed pre-Permian Sequence that had dips of 85º (Figure 16). The exposed Hajar Supergroup that flanks the pre-Permian Sequence does not show extreme deformation, but instead has gently dipping strata (about 15ºS) on the southern limb of Jebel Akhdar and steeper dipping strata (about 28ºN) on its northern limb. Also, gravity modeling shows considerable thinning of the pre-Permian Sequence in the northern limb of Jebel Akhdar. This sudden decrease in the pre-Permian Sequence thickness on the northern limb may be associated with the Permian rifting event that formed the eastern margin of the Arabian Plate. Also shown in Figure 16 is the considerable load of the Semail Ophiolite and the Hawasina Sediments that occurs north of the mountain and which possibly contributed to the steepness of the northern limb of the mountains. A density thickness trade-off exists between the ophiolite and the Hawasina Sediments in the Coastal Zone.

With regard to question 3, based on the interpretation of Figures 9 and 10 we infer a major uplift episode starting in the Late Oligocene and confirmed by several other observations. In line IUL0205 (Figure 10) north of Jebel Akhdar, the seismic stratigraphy shows strata of the Alkhawd Formation and the Hadhramout Group (Tertiary Cover Sequence) dipping north at 25º to 30º. This observation provides a Late Oligocene date for the episodic uplift of the Oman Mountains and is in agreement with fission track dating by Mount et al. (1998) of the uplift of the Jebel Akhdar anticline. Moreover, seismic data in the Hamrat Ad Duru Zone (Figure 9) show southerly dipping reflectors of the Fiqa Formation forming downlaps as the result of the continued uplift of the mountains. This indicates that the mountain uplift continued after the Maastrichtian, that is, after the deposition of the Fiqa. The uplift also affected the Interior Zone with a lesser magnitude than in the Hamrat Ad Duru and Mountain zones.

In summary, the uplift and unroofing of the Oman Mountains possibly started in the Late Cretaceous as indicated by the intermontane deposits of the Alkhawd Formation and its equivalent in the Coastal Zone (Figure 10). The major uplift began in the Late Oligocene and was probably related to tectonic events on the nearby plate boundaries of the Zagros collision zone and the Makran subduction system. The Cretaceous-Tertiary boundary is an important marker but due to the lack of information, especially of well data, we were unable to cover it adequately in our discussion of the Foreland region and the Coastal Zone. However, it is important to determine the continuity or absence of this unconformity in the subsurface of the Coastal Zone.

Finally, the offshore area shows the development of an extensive Tertiary sedimentary basin (Oligocene-Holocene) that could be the extension of the Sohar basin of Ravaut et al. (1998). The basin extends northward for approximately 60 km at the northern end of the crustal model (Figure 16). The basin is deepest, about 7 km below sea level, in the vicinity of the present-day shoreline. The seismic section in the offshore area is primarily characterized by gravity faults (Figure 16).

CONCLUSIONS

The four main results of this study are as follows: (1) The eastern Arabian continental crust has an average thickness of about 40 km in the Foreland region, is about 50 km thick beneath Jebel Akhdar, and about 35 km beneath the Coastal Zone. (2) Based on gravity modeling, the pre-Permian Sequence in the core of Jebel Akhdar is estimated to be about 9 km thick. This observation conforms well with most structural models of the Jebel Akhdar range that require thickening, either by duplexing, blind thrust faulting, or decollement below the core and the southern limb of Jebel Akhdar. (3) Based on surface and subsurface observations and gravity modeling, the Nakhl Ophiolite block extends beyond the shoreline for approximately 80 km from its most southerly surface outcrop. The Nakhl block averages 5 km in thickness, whereas the ophiolite body south of the Jebel Akhdar range has a maximum thickness of only 1 km. The underlying unit of the Hawasina Sediments has an average thickness of between 2 and 3 km in the Hamrat Ad Duru Zone and 2 km in the Coastal Zone. (4) Basement-related wrench faults in the Foreland region strike northwest and are predominantly transtensional. They often offset preexisting structures such as the Salakh-Madmar range. We conclude that no major compressional events took place during the Tertiary within the Foreland region.

ACKNOWLEDGMENTS

We thank the Oman Ministry of Oil and Gas for allowing us access to seismic reflection and well data, and to the Department of Minerals for their support and for providing gravity data. We also thank Petroleum Development Oman for assistance in obtaining seismic reflection and well data. The receiver function data were provided by the Department of Earth Sciences, Sultan Qaboos University, Muscat, Oman and the recorded data are from the Earthquake Monitoring Project under the leadership of Waris Warsi. Our special thanks go to Samir Hanna, Department of Earth Sciences, Sultan Qaboos University, and to our colleagues at Cornell University—Graham Brew, Francisco Gomez, Alexander Calvert, Marisa Vallve, Carrie Brindisi, Christine Sandvol, David Steer, and Khaled Al-Damegh—for their helpful advice and comments. We thank the two anonymous referees for their constructive reviews and the *GeoArabia* editors for improving the manuscript. The design and drafting of the final graphics was by Gulf PetroLink.

REFERENCES

Al-Harthy, M.S., R.G. Coleman, M.W. Hughes-Clarke and S.S. Hanna 1991. Tertiary basaltic intrusions in the Central Oman Mountains. In, T.J. Peters, A. Nicolas and R.G. Coleman (Eds.), Ophiolite Genesis and Evolution of the Oceanic Lithosphere. Ministry of Petroleum and Minerals, Sultanate of Oman, p. 675–682.

Badri, M. 1990. Crustal structure of central Saudi Arabia determined from seismic refraction profiles. Tectonophysics, v. 185, no. 3–4, p. 357–374.

Bechennec, F., M. Beurrier, G. Hutin and D. Rabu 1986a. Geological map of Barka. Ministry of Petroleum and Minerals, Sultanate of Oman.

Bechennec, F., M. Beurrier, G. Hutin and D. Rabu 1986b. Geological map of Bahla. Ministry of Petroleum and Minerals, Sultanate of Oman.

Bechennec, F., J. Le Métour, J-P. Platel and J. Roger 1995. Doming and down-warping of the Arabian Platform in Oman in relation to Eoalpine tectonics. In, M.I. Al-Husseini (Ed.), Middle East Petroleum Geosciences, GEO'94. Gulf PetroLink, Bahrain, v. 1, p. 167–178.

Beurrier, M., F. Bechennec, G. Hutin and D. Rabu 1986. Geological map of Rustaq. Ministry of Petroleum and Minerals, Sultanate of Oman.

Boote, D.R.D., D. Mou and R.I. Waite 1990. Structural evolution of the Suneinah foreland, central Oman Mountains. In, A.H.F. Robertson, M.P. Searle and A.C. Ries (Eds.), The Geology and Tectonics of Oman Region. Geological Society, London, Special Publication no. 49, p. 397–418.

Boudier, F. and R.G. Coleman 1981. Cross-section through the peridotite in the Semail Ophiolite, southeastern Oman Mountains. Journal of Geophysical Research, v. 86, no. B4, p. 2573–2592.

Boudier, F., J.L. Bouchez, A. Nicolas, M. Cannat, G. Ceuleneer, M. Misseri and R. Montigny 1985. Kinematic of oceanic thrusting in the Oman Ophiolite: model for plate convergence. Earth and Planetary Sciences Letters, v. 75, p. 215–222.

Burdick, L.J. and A.C. Langston 1977. Modeling crustal structure through the use of converted phases in teleseismic body-wave forms. Bulletin of the Seimological Society of America, v. 67, no. 3, p. 677–691.

Cassidy, J.F. 1992. Numerical experiments in broadband receiver function analysis. Bulletin of the Seimological Society of America, v. 82, no. 3, p. 1453–1474.

Cawood, P.A., F.K. Green and T.J. Calon 1990. Origin of culmination within the southeast Oman Mountains at Jebel Majhool and Ibra Dome. In, A.H.F. Robertson, M.P. Searle and A. C. Ries (Eds.), The Geology and Tectonics of the Oman Region. Geological Society, London, Special Publication no. 49, p. 429–445.

Chevrel, S., F. Bechennec, J. Le Métour, J. Roger and R. Wyns 1992. Geological map of Jubuayl Fahud. Ministry of Petroleum and Minerals, Sultanate of Oman.

Christensen, N.I. and J.D. Smewing 1981. Geology and seismic structure of the northern section of the Oman Ophiolite. Journal of Geophysical Research, v. 86, no. B4, p. 2545–2555.

Clayton, R.W. and R.A. Wiggins 1976. Source shape estimation and deconvolution of teleseismic body waves. Geophysical Journal of the Royal Astronomical Society, v. 47, p. 151–177.

Coleman, R.G. 1981. Tectonic setting for ophiolite obduction in Oman. Journal of Geophysical Research, v. 86, no. B4, p. 2497–2508.

El-Shazly, A.K. and R.G. Coleman 1990. Metamorphism in the Oman Mountains in relation to the Semail Ophiolite emplacement. In, A.H.F. Robertson, M.P. Searle and A.C. Ries (Eds.), The Geology and Tectonics of the Oman Region. Geological Society, London, Special Publication no. 49, p. 473–493.

Gardner, G.H., L.W. Gardner and A.R. Gregory 1974. Formation velocity and density—the diagnostic basis for stratigraphic traps. Geophysics, v. 39, p. 770–780.

Glennie, K.W., M.G.A. Boeuf, M.W. Hughes Clarke, M. Moody-Stuart, W.F.H. Pilaar and B.M. Reinhardt 1973. Late Cretaceous nappes in Oman mountains and their geologic evolution. American Association of Petroleum Geologists Bulletin, v. 57, p. 5–26.

Hanna, S.S. 1990. The Alpine deformation of the central Oman Mountains. In, A.H.F. Robertson, M.P. Searle and A.C. Ries (Eds.), The Geology and Tectonics of the Oman Region. Geological Society, London, Special Publication no. 49, p. 341–359.

Hanna, S.S. and S.C. Nolan 1989. The Maradi fault zone: evidence of late Neogene tectonics in the Oman Mountains. Journal of the Geological Society, London, v. 146, p. 867–871.

Hanna, S.S. and J.D. Smewing 1996. The stratigraphy and structure of the Madamar-Salakh-Qusaybah range and Natih-Fahud area in the Oman Mountains. Journal of Science and Technology, Sultan Qaboos University, Oman, v. 1, p. 1–19.

Hopson, C.A., R.G. Coleman, R.T. Gregory, J.S. Pallister and E.H. Baily 1981. Geologic section through the Semail Ophiolite and associated rocks along the Muscat-Ibra transect, southeastern Oman Mountains. Journal of Geophysical Research, v. 86, p. 2527–2544.

Le Métour, J., F. Bechennec and J. Roger 1995. Late Permian birth of the Neo-Tethys and development of its southern continental margin in Oman. In, M.I. Al-Husseini (Ed.), Middle East Petroleum Geosciences, GEO'94. Gulf PetroLink, Bahrain, v. 2, p. 643–654

Le Métour, J., J.C. Michel, F. Bechennec, J.P. Platel and J. Roger 1995. Geology and mineral wealth of the Sultanate of Oman. Ministry of Petroleum and Minerals, Sultanate of Oman, 285 p.

Lippard, S.J. 1983. Cretaceous high pressure metamorphism in NE Oman and its relation to subduction and ophiolite nappe emplacement. Journal of the Geological Society, London, v. 140, p. 97–104.

Manghnani, M.H. and R.G. Coleman 1981. Gravity profiles across the Semail Ophiolite, Oman. Journal of Geophysical Research, v. 86, no. B4, p. 2509–2525.

Mann, A. and S.S. Hanna 1990. The tectonic evolution of pre-Permian rocks, central and southeastern Oman Mountains. In, A.H.F. Robertson, M.P. Searle and A.C. Ries (Eds.), The Geology and Tectonics of the Oman Region. Geological Society, London, Special Publication no. 49, p. 307–325.

Mattes, B.W. and S.C. Morris 1990. Carbonate/evaporite deposition in the late Precambrian-Early Cambrian Ara Formation of Southern Oman. In, A.H.F. Robertson, M.P. Searle and A.C. Ries (Eds.), The Geology and Tectonics of the Oman Region. Geological Society, London, Special Publication no. 49, p. 617–636.

Michard, A., J.L. Bouchez and M. Ouazzani-Touhami 1984. Obduction-related planar and linear fabrics in Oman. Journal of Structural Geology, v. 6, p. 39–49.

Mooney, W.D., M.E. Gettings, H.R. Blank and J.H. Healy 1985. Saudi Arabian seismic-refraction profile: a travel-time interpretation of crustal and upper mantle structure. Tectonophysics, v. 111, p. 173–246.

Mount, V.S., R.I.S. Crawford and S.C. Bergman 1998. Regional structural style of the central and southern Oman Mountains: Jebel Akhdar, Saih Hatat, and the northern Ghaba Basin. GeoArabia, v. 3, no. 4, p. 475–489.

Naylor, M.A. and L.Y. Spring 2001. Exploration strategy, development and performance management: a portfolio-based approach. GeoArabia, v. 6, no. 4, p. 553–570.

Nicolas, A., F. Boudier and B. Ildefonse 1996. Variable crustal thickness in the Oman ophiolite: implication for oceanic crust. Journal of Geophysical Research, v. 101, no. B8, p. 17,941–17,950.

Nolan, S.C., P.W. Skelton, B.P. Clissold and J.D. Smewing 1990. Maastrichtian to early Tertiary stratigraphy and palaeogeography of the central and northern Oman Mountains. In, A.H.F. Robertson, M.P. Searle and A.C. Ries (Eds.), The Geology and Tectonics of the Oman Region. Geological Society, London, Special Publication no. 49, p. 495–519.

Pallister, J.S. and C.A. Hopson 1981. Semail ophiolite plutonic suite: field relations, phase variation, cryptic variation and layering, and model for a spreading ridge magma chamber. Journal of Geophysical Research, v. 86, no., B4, p. 2,593–2,644.

Pratt, B.R. and J.D. Smewing 1990. Jurassic and Early Cretaceous platform margin configuration and evolution, central Oman Mountains. In, A.H.F. Robertson, M.P. Searle and A.C. Ries (Eds.), The Geology and Tectonics of the Oman Region. Geological Society, London, Special Publication no. 49, p. 69–88.

Rabu, D., F. Bechennec, M. Beurrier and G. Hutin 1986. Geological map of Nakhl. Ministry of Petroleum and Minerals, Sultanate of Oman.

Ravaut, P. 1997. Les anomalies de pesanteur en Oman: implications sur la structure et l'evolution tectonique de la chaine nord-omanaise. Unpublished PhD dissertation, Montpellier University, France, 255 p.

Ravaut, P. and W. Warsi 1997. Bouguer anomaly map of Oman. Ministry of Petroleum and Minerals, Sultanate of Oman.

Ravaut, P., R. Bayer, R. Hassani, D. Rousset and A.A. Yahya'ey 1997. Structure and evolution of the northern Oman margin: gravity and seismic constraints over the Zagros-Makran-Oman collision zone. Tectonophysics, v. 279, p. 253–280.

Ravaut, P., D. Carbon, J-F. Ritz, R. Bayer and H. Philip 1998. The Sohar basin, western Gulf of Oman: description and mechanisms of formation from seismic and gravity data. Marine and Petroleum Geology, v. 15, no. 4, p. 359–377.

Robertson, A. 1987. The transition from a passive margin to an Upper Cretaceous foreland basin related to ophiolite emplacement in the Oman Mountains. Geological Society of America Bulletin, v. 99, no. 11, p. 633–653.

Sandvol, E., D. Seber, A. Calvert and M. Barazangi 1998. Grid search modeling of receiver functions: implications for crustal structure in the Middle East and North Africa. Journal of Geophysical Research, v. 103, no. B11, p. 26,899–26,917.

Sandvol, E., D. Seber, M. Barazangi, F. Vernon, R. Mellors and A. Al-Amri 1998. Lithospheric seismic velocity discontinuities beneath the Arabian Shield. Geophysical Research Letters, v. 25, no. 15, p. 2,873–2,876.

Searle, M. and J. Cox 1999. Tectonic setting, origin, and obduction of the Oman ophiolite. Geological Society of America Bulletin, v. 111, no. 1, p. 104–122.

Sharland, P.R., R. Archer, D.M. Casey, R.B. Davies, S.H. Hall, A.P. Heward, A.D. Horbury and M.D. Simmons 2001. Arabian Plate Sequence Stratigraphy. GeoArabia Special Publication 2, Gulf PetroLink, Bahrain, 371 p.

Shelton, A.W. 1990. The interpretation of gravity data in Oman: constraints on the ophiolite emplacement mechanism. In, A.H.F. Robertson, M.P. Searle and A.C. Ries (Eds.), The Geology and Tectonics of the Oman Region. Geological Society, London, Special Publication no. 49, p. 459–471.

Warbuton, J., T.J. Burnhill, R.H. Graham and K.P. Isaac 1990. The evolution of the Oman Mountains foreland basin. In, A.H.F. Robertson, M.P. Searle and A.C. Ries (Eds.), The Geology and Tectonics of Oman Region. Geological Society, London, Special Publication no. 49, p. 419–427.

Wyns, R., F. Bechennec, S. Chevrel, J. Le Métour, and J. Roger 1992. Geological map of Nazwa. Ministry of Petroleum and Minerals, Sultanate of Oman.

Zandt, G. and C.J. Ammon 1995. Continental crust composition constrained by the measurement of the crustal Poisson's ratio. Nature, v. 374, no. 9, p. 152–154.

ABOUT THE AUTHORS

Ali I. Al-Lazki *is a member of the Department of Earth Sciences at Sultan Qaboos University, Muscat, Oman. He is currently working toward a PhD in Earthquake Seismology and Geophysics at Cornell University under the direction of Prof. Muawia Barazangi. He has a BSc in Earth Sciences from Sultan Qaboos University, and an MSc in Geophysics (studying the effect of clay content on AVO response in a sandstone reservoir) from the University of Tulsa. Ali's present research interest is in the integration of regional-scale geological, geophysical, and seismological data.*

E-mail: aiaz@cornell.edu

Dogan Seber *is a Senior Research Associate in the Institute for the Study of the Continents at Cornell University. He has a BS in Geophysics from Istanbul Technical University, an MS in Seismology from St. Louis University, and a PhD in Seismology from Cornell University. Dogan's doctoral research was on the analysis and interpretation of seismic and gravity data for determining the crustal and lithospheric structure of the Atlas and Rif Mountains in Morocco and the Palmyrides Mountains in Syria. He has recently developed a digital seismological, geophysical, and geological database for the Middle East and North Africa that can be analyzed with menu-driven access tools via a specially designed web server.*

E-mail: seber@cornell.edu

Eric Sandvol *is a Research Scientist in the Institute for the Study of the Continents at Cornell University. He has a BS in Physics from South Dakota School of Mines & Technology and a PhD in Physics and Seismology from New Mexico State University. His doctoral research involved the observation and interpretation of mantle seismic anisotropy in Pakistan, Tibet, the Rio Grande rift, and the Japan subduction zone. Eric is currently researching waveform analysis as a means of characterizing crustal and upper mantle seismic velocity and attenuation in the Middle East and North Africa.*

E-mail: sandvol@cornell.edu

Muawia Barazangi *is a Professor in the Department of Geological Sciences at Cornell University. He is also Associate Director of the Institute for the Study of the Continents, and leader of the Cornell Middle East Project. Muawia has a BS in Physics and Geology from Damascus University, an MS in Geophysics from the University of Minnesota, and a PhD in Seismology from Columbia University's Lamont-Doherty Earth Observatory. His research interests include global tectonics, seismotectonics of continental collision zones, intracontinental mountain belts, and tectonics of the Middle East.*

Corresponding author: Institute for the Study of the Continents, Cornell University, Snee Hall, Ithaca, New York 14853, USA
E-mail: mb44@cornell.edu

Manuscript Received March 24, 2001

Revised July 16, 2001

Accepted July 29, 2001